Doctoral Dissertation
博士論文

Physiological functions of neurosteroids produced by steroid 7α-hydroxylase CYP7B1 in mice

(ステロイド 7α水酸化酵素 CYP7B1 により合成される マウスニューロステロイドの生理機能解析)

A Dissertation Submitted for Degree of Doctor of Philosophy
January 2019

平成 31 年 1 月　博士 (理学) 申請

Department of Biophysics and Biochemistry,
Graduate School of Science, The University of Tokyo

東京大学大学院理学系研究科生物化学専攻

Kanako MAEHATA

前畑　佳納子

Abstract

Neuroactive steroids, termed neurosteroids, are synthesized *de novo* in the brain and influence biological functions including behavior and higher brain function. These neurosteroids are synthesized from cholesterol by a series of enzymes, among which one of the P450 hydroxylases, cytochrome P450-7b1 (CYP7B1), catalyzes formation of 7-hydroxylated neurosteroids, 7α-hydroxypregnenolone (7α-OH-Preg) and 7α-hydroxydehydroepiandrosterone (7α-OH-DHEA). In this study, I found higher levels and diurnal expression of *Cyp7b1* mRNA in the mouse hippocampus among various brain regions, and identified 7α-OH-Preg and 7α-OH-DHEA in the mouse hippocampal extract by using ultra-performance liquid chromatography coupled with electrospray-tandem mass spectrometry in negative ion mode. This is the first report to identify these steroids in the mouse brain without derivatization for mass spectrometry. Then, I investigated behavioral phenotype of *Cyp7b1*-deficient mice. Intriguingly, *Cyp7b1*-deficiency did not affect recent memory but impaired remote memory in the Morris water maze test. Furthermore, chronic intracerebroventricular administration of a mixture of 7α-OH-Preg and 7α-OH-DHEA improved remote spatial memory performance of *Cyp7b1*-deficient mice. These results demonstrate that the 7α-hydroxylated neurosteroids regulate long-term maintenance of spatial memory in mice.

Contents

1. Introduction 1

2. Materials and methods 4

3. Results 13

4. Discussion 21

5. Conclusion 26

6. References 27

7. Figures and Table 31

8. Acknowledgements 48

1. Introduction

Neurosteroids are neuroactive steroids that are synthesized *de novo* in the brain (Corpéchot *et al.*, 1981; Akwa *et al.*, 1992) and regulate various biological functions including behaviors and higher brain functions, *e.g.* cognition or emotion (Baulieu *et al.*, 2000; Kihel *et al.*, 2012; Tsutsui *et al.*, 2013, 2018; Wingfield *et al.*, 2018). At the first step of steroidogenesis, neurosteroids are synthesized from cholesterol, which is transferred from the outer to the inner mitochondrial membrane by steroidogenic acute regulatory protein (StAR) (Figure 1). Then cholesterol is converted into pregnenolone, a common precursor of neurosteroids, by cholesterol monooxygenase (CYP11A1; termed also P450scc, cholesterol side chain cleavage enzyme) (Figure 1). Pregnenolone is subsequently converted into a variety of bioactive steroids by hydroxylation and/or oxidation (Akwa *et al.*, 1992; Morfin *et al.*, 1994; Payne *et al.*, 2004; Wingfield *et al.*, 2018). As one of the conversion pathways, cytochrome P450-7b1 (CYP7B1) catalyzes hydroxylation of pregnenolone at the 7α-position, and synthesizes a less characterized neurosteroid, 7α-hydroxypregnenolone (7α-OH-Preg) (Akwa *et al.*, 1992). CYP7B1 is essential for biosynthesis of 7α-OH-Preg in the brain (Rose *et al.*, 1997).

7α-OH-Preg was identified in the brain extract of male newts in breeding period as a compound that stimulates locomotor activity (Matsunaga *et al.*, 2004). Subsequently it was found that 7α-OH-Preg increases locomotor activity also in quail and is synthesized in a time-of-day-dependent manner (Tsutsui *et al.*, 2008; Koyama *et al.*, 2009). Then, in chicken, it was revealed that 7α-OH-Preg is secreted from the pineal gland and a light pulse given at early subjective night activates the pineal production of 7α-OH-Preg and locomotor activity of chicken (Hatori

et al., 2011). On the other hand, 7α-OH-Preg has not been identified in the rodent brain. However, it was reported that intracerebroventricular infusion of 7α-OH-Preg into aged rats ameliorates the spatial memory impairment (Yau *et al.*, 2006), and *Cyp7b1* mRNA, which is considered to be needed for biosynthesis of 7α-OH-Preg (Rose *et al.*, 1997), is expressed widely in rodent tissues, with the higher levels in the liver, kidney and hippocampus (dentate gyrus) (Rose *et al.*, 2001).

7α-Hydroxy-dehydroepiandrosterone (7α-OH-DHEA) is another neurosteroid synthesized by CYP7B1 (Rose *et al.*, 1997). In biosynthesis of 7α-OH-DHEA, pregnenolone is firstly converted into dehydroepiandrosterone (DHEA) by CYP17A1, and then DHEA is 7α-hydroxylated by CYP7B1 to form 7α-OH-DHEA (Figure 1). 7α-OH-DHEA was identified in the ventricular cerebrospinal fluid of human with hydrocephalus (Stárka *et al.*, 2009). Although 7α-OH-DHEA has not been detected in the rodent brain, 7α-hydroxylating activity on DHEA is demonstrated by *ex viv*o assays among a variety of tissues including the brain (Morfin *et al.*, 1994; Rose *et al.*, 2001). 7α-OH-DHEA has neuroprotective effect on ischemia-induced rat hippocampal neurons in culture (Pringle *et al.*, 2003).

In addition, *Cyp7b1* mRNA is significantly reduced in the dentate neurons from Alzheimer's disease subjects (Yau *et al.*, 2003), and CYP7B1 bioactivity is decreased in the hippocampus of cognitively impaired aged rats (Yau *et al.*, 2006). Therefore, CYP7B1 and/or its products are considered to be relevant to higher brain functions particularly to hippocampus-dependent memory performance in mammals.

In this study, to elucidate the physiological roles of the 7α-hydroxylated neurosteroids in mammals, I investigated existence of these neurosteroids

in the mouse brain and behavioral phenotype of *Cyp7b1* KO mice, which should have no ability to synthesize 7α-hydroxylated steroids in the brain. Then, I revealed that *Cyp7b1* KO mice show impaired long-term maintenance of spatial memory, and it was ameliorated by intracerebroventricular infusion of 7α-hydroxylated steroids.

2. Materials and Methods

Animals

Adult male mice were housed under 12 hr light/12 hr dark cycle (LD) with the light provided by white fluorescent lamps (300-400 lx at the level of the heads of mice) in a light-tight chamber at 23 °C ± 1 °C and constant humidity (55% ± 10%) in cages with commercial chow (CLEA Japan, Inc.) and water available *ad libitum*. The time point when the light turned on was defined as zeitgeber time (ZT) 0 and the turned off as ZT12. For behavioral experiments, adult male mice (7-15 weeks) were housed individually in their home cages, and handled daily for at least one week before all the tests. All animal experiments were performed in accordance with the guidelines of The University of Tokyo.

Cyp7b1 knockout mice in a mixed C57BL/6J × 129 genetic background (Li-Hawkins *et al.*, 2000) were obtained from The Jackson Laboratory. The mice were bred to C57BL/6J for at least one generation at The Jackson Laboratory. After arrival at our laboratory, they were bred to C57BL/6J for three generations. In this mutant, deletion of exon 6 of the *Cyp7b1* gene eliminated CYP7B1 protein and its enzyme activity completely (Li-Hawkins *et al.*, 2000). Some studies have shown that lack of *Cyp7b1* may cause defects in reproductive behaviors (Oyola *et al.*, 2015) or proliferation (Rose *et al.*, 2001; Omoto *et al.*, 2005), but in our laboratory, *Cyp7b1* KO mice were fertile and apparently indistinguishable from WT mice.

RNA extraction and RT-qPCR

Total RNA was extracted by TRIzol reagent (Invitrogen) and purified from the pineal glands and the prefrontal cortexes by using RNeasy MinElute Cleanup Kit (Qiagen) or from the other brain tissues by using RNeasy Mini Kit (Qiagen)

according to the manufacturer's protocol. The RNA was reverse-transcribed into complementary DNA (cDNA) using the oligo $(dT)_{15}$ primer with GoScript Reverse Transcriptase (Promega). The cDNA was subjected to quantitative PCR using GoTaq qPCR Master Mix (Promega) with the StepOnePlus Real-time PCR system (Applied Biosystems) according to the manufacturer's protocol. The mRNA levels were quantified in a relative standard curve method. The standard samples were liver cDNA for *Cyp7a1*, pineal cDNA for arylalkylamine-N-acetyltransferase (*Aanat*), and hippocampal cDNAs for the other genes. The gene-specific primers used for RT-qPCR were *StAR*-Fw (5'-GCTGG AAGCT CCTAT AGACA-3'), *StAR*-Rv (5'-AGCTC CGACG TCGAA CTTGA-3'), *Cyp11a1*-Fw (5'-ACATG GCCAA GATGG TACAG TTG-3'), *Cyp11a1*-Rv (5'-ACGAA GCACC AGGTC ATTCA C-3'), *Cyp7b1*-Fw (5'-CGGAA ATCTT CGATG CTCC-3'), *Cyp7b1*-Rv (5'-TAGCC CTATA GGCTT CCTGT CG-3'), *Cyp17a1*-Fw (5'-TGACC AGTAT GTAGG CTTCA GTCG-3'), *Cyp17a1*-Rv (5'-TCCTT CGGGA TGGCA AACTC TC-3'), *Cyp7a1*-Fw (5'-AGCAA CTAAA CAACC TGCCA GTAC-3'), *Cyp7a1*-Rv (5'-GTCCG GATAT TCAAG GATGC A-3'), *Aanat*-Fw (5'-ATCAC CGTGG GCTCT CTCAC C-3'), *Aanat*-Rv (5'-GCCAT GGCCA AGCAC ACAG-3'), *Dbp*-Fw (5'-AATGA CCTTT GAACC TGATC CCGCT-3'), *Dbp*-Rv (5'-GCTCC AGTAC TTCTC ATCCT TCTGT-3'), *Rps29*-Fw (5'-TGAAG GCAAG ATGGG TCAC-3'), and *Rps29*-Rv (5'-GCACA TGTTC AGCCC GTATT-3').

Extraction and purification of steroids

Hippocampi isolated from four or five male mice after following behavioral analysis were homogenized in ten volumes of Hanks' balanced salt solution (1 mL) with a glass-Teflon homogenizer on ice. Steroids were extracted by an equivalent volume of ethyl acetate (1 mL) three times, and the extracts collected

in glassware were evaporated under a gentle stream of nitrogen. The dried extract was dissolved in 0.4 mL of methanol/H_2O (75/25, v/v) three times, collected in a 1.5 mL-tube and then centrifuged (3,000 × *g*, 5 min). The supernatant was diluted with H_2O to a final concentration of 37.5 % methanol and subjected to purification with a solid-phase extraction column (Bond Elut Plexa, 200 mg, 6 mL; Agilent), which had been pre-washed with methanol (5 mL) and methanol/H_2O (75/25, v/v; 4 mL) and equilibrated with methanol/H_2O (37.5/62.5, v/v; 6 mL) successively. The sample was loaded on the column and the flow-through fraction was discarded. The column was then washed with methanol/H_2O (37.5/62.5, v/v; 6 mL), and the steroid fraction was eluted with methanol/H_2O (75/25, v/v; 3 mL) and evaporated under a gentle stream of nitrogen or under vacuum.

Liquid chromatography

Standard mixture (7α-OH-Preg, 7α-OH-DHEA, pregnenolone and DHEA, 100 ng each) were analyzed by using an Agilent 1260 Infinity LC system (Waldbronn, Germany) consisting of a binary pump, a micro vacuum degasser, a temperature controlled auto-sampler, a column oven, and a diode array detector. The sample storage temperature was 6 °C. The stationary phase was an Inertsil ODS-3 2.1 mm×150 mm, 3 μm column (GL Science), which was maintained at 25 °C. The sample was dissolved in acetonitrile/H_2O (30/70, v/v; 20 μL) and centrifuged (13,500 rpm, 4 °C, 15 min), and 5 μL of the supernatant was injected. The mobile phase consisted of H_2O and acetonitrile. The column was eluted with a 40-min linear gradient of 30-70% acetonitrile at a flow rate of 0.15 mL/min. The steroids were detected by absorbance at 200 nm.

Liquid chromatography-mass spectrometry

7α-OH-Preg and 7α-OH-DHEA were analyzed by using an Agilent 1290 Infinity II LC system (Waldbronn, Germany) consisting of a binary pump, a micro vacuum degasser, a temperature controlled auto-sampler and a column oven. The sample storage temperature was 4 °C. The stationary phase was an Agilent Poroshell Phenyl Hexyl 2.1 mm×10 mm, 2.7 μm column, which was maintained at 40 °C. The sample was dissolved in acetonitrile/H_2O (20/80, v/v; 12 μL), and 10 μL of the reconstituted sample was injected and eluted at a flow rate of 0.4 mL/min. The mobile phase consisted of 0.4 mM NH_4F in H_2O (solvent A) and acetonitrile/methanol (1/1, v/v; solvent B). The elution gradient was maintained at 1 % B for the first 4.2 min, 1.0-35.0 % B from 4.2 to 5.5 min, 35.0-95.0 % B from 5.5 to 12 min, 95.0-1.0 % from 12.0 to 12.1 min and held at 1 % B from 12.1 to 16.0 min. Mass spectrometry experiments were performed with electrospray ionization (ESI) in negative ion mode by using an Agilent 6470 Triple Quad MS system. The capillary voltage was -3,500 V. The gas temperature was maintained at 210 °C. The sheath gas temperature was 375 °C and the flow rate was 12 L/min. The nebulizer gas flow was 13 L/min. Multiple reaction monitoring (MRM) was applied for highly selective and sensitive detection of 7α-OH-Preg and 7α-OH-DHEA. Three different MRM transitions were set and optimized for each steroid as shown in Table 1.

Locomotor activity

Male mice were housed individually in cages equipped with infrared area sensors (Elekit). Mice were entrained to a light-dark (LD) cycle for at least four weeks and released into constant darkness (DD). The total activities were recorded in five-min bins and analyzed with ClockLab analysis software (Actimetrics). The circadian period of the activity rhythms in DD was

determined by using an extrapolation procedure with ClockLab. The time points of the onsets of mice activity were defined as circadian time (CT) 12. Mice were exposed to a 30-min light pulse (white light; 300-400 lx) at CT22 or CT14. Activity onsets were calculated by ClockLab to quantify the light-induced phase shift.

Elevated plus maze test

The elevated plus maze (EPM) was constructed of Plexiglas (O'Hara & Co., Tokyo, Japan) with two open arms (25 cm×5 cm) and two enclosed arms with clear walls (15 cm height) at an elevation of 50 cm above the floor. The arms of the maze form a cross with the two open arms facing each other. The maze was washed and dried after each test. A male mouse was placed on the center of the maze facing one of the closed arms under a light of 4.0 lx ± 0.1 lx (flat white LED). The behavior was recorded for 5 min by a video camera positioned above the maze. The rate of recording: 4 frame/s, moving criterion: 3 cm.

The numbers of entries into the open and closed arms and the time spent exploring the open and closed arms were analyzed using a computer-operated system (TimeEP1; O'Hara & Co., Tokyo, Japan).

Open field test

A male mouse was placed in the right front corner of a white Plexiglas open field arena (40 cm×40 cm, 30 cm height) (O'Hara & Co., Tokyo, Japan) and allowed to explore for 5 min under a light of 330 lx ± 10 lx (flat white LED). The arena was cleaned up with disinfectant spray and water spray in this order after each test. The activity in the open field was recorded by a video camera positioned above the arena using a computer-operated system (OpenField

plug-in; O'Hara & Co., Ltd.), a modified software based on the public domain Image J program (developed at the U.S. National Institutes of Health and available on the Internet at http://rsb.info.nih.gov/ij). Total distance and the time spent in the center area of the arena were calculated. The rate of recording: 3 frame/s, center area: 30%.

Forced swim test

A male mouse was placed in a Plexiglas beaker (22 cm×∅12 cm) (O'Hara & Co., Tokyo, Japan) containing water 15 cm in depth at 24 °C ± 1 °C for 5 min under a light of 4.0 lx ± 0.1 lx (flat white LED) from underneath. The beaker was washed and water was changed after each test. All tests were recorded by a video camera positioned above the beaker. The total distance of swimming and the immobility time were analyzed by using a computer-operated system (TimeFZ; O'Hara & Co., Tokyo, Japan). The rate of recording: 4 frame/s, freezing criterion: 800 pixel, freezing duration: 3 sec.

Intracerebroventricular injection of steroids for forced swim test

A male mouse was anesthetized by an intraperitoneal injection (20 μL/g body weight) of a mixture of ketamine (4.4 mg/mL; Daiichi Sankyo Propharma) and xylazine (0.44 mg/mL; Bayer Health Care) dissolved in bacteriostatic saline and placed in a stereotaxic frame (Narishige Inc.) keeping bregma and lambda at a horizontal level. A small hole was drilled in the skull on the right lateral ventricle using the following coordinates relative to bregma: 0.22 mm posterior; 1.0 mm right lateral. All mice were handled for at least one week before the surgery, housed individually after the surgery and allowed to recover from the surgery for at least one week.

A mouse was anesthetized by exposure to isoflurane and injected with steroids. Steroids were dissolved in 1 μL of artificial CSF (aCSF) with 1% DMSO. aCSF was prepared at time of use by mixing the same volume of solvent A containing 150 mM NaCl, 3 mM KCl, 1.4 mM $CaCl_2$, 0.8 mM $MgCl_2$ and solvent B containing 0.8 mM Na_2HPO_4, 0.2 mM NaH_2PO_4, and pH was adjusted at 7.4 with NaOH. The concentration of 7α-OH-Preg (Steraloids Inc.) or 7α-OH-DHEA (Steraloids Inc.) solution; 100 ng/μL. Mixed steroid solution; 50 ng/μL each of 7α-OH-Preg and 7α-OH-DHEA. Each injection was made over a period of 2 min at a rate of 0.5 μL/min using 30 G blunt-tip needle connected with a catheter to a syringe pump. The needle was positioned 2.3 mm below from the small hole and left in the place for additional 30 seconds after each injection to allow for diffusion of the steroids.

Forced swimming tests were carried out, 10 minutes after the injection.

Morris water maze test

The Morris water maze test was performed in a white Plexiglas circular pool (30 cm height, ∅ 100 cm; O'Hara & Co., Tokyo, Japan), which was set at a fixed position apart from the room walls or curtains, filled to a depth of 21 cm with water at 24 ± 1 °C and made opaque by adding TiO_2. A circular escape platform (20 cm height, ∅ 10 cm) was placed 1.0 cm below the water surface at a fixed position in a goal quadrant. All the tests were performed under a flat white LED light at 4.0 lx ± 0.1 lx. The day before water maze training, a mouse was placed on the platform in an equilateral triangle frame (40 cm on a side, 45 cm in height) for 3 min without any visible cues for the purpose of the habituation to the platform.

A male mouse was trained for consecutive five days with four trials per day. On each training trial, a start position was selected randomly from one of the three start positions at the pool edge of three quadrants (right, left, and opposite to the goal quadrant). The mouse was gently placed in the water facing the wall. The trial was completed once the mouse found the hidden platform. If the mouse failed to find the platform within 60 sec on a given trial, the experimenter gently guided the mouse onto the platform. Male mice of *Cyp7b1* KO and the littermate WT were divided into two groups (for the two time points, ZT1 and ZT11.5) each composed of 12-16 individuals. The mice were trained at ZT1 or ZT11.5 with four training trials at three to seven min inter-trial intervals per day.

On the next day of the last training, spatial memory was assessed in a probe test (probe test I), in which the platform was removed from the pool. The mouse was allowed 60 sec to search for it, and the time when the mouse stayed in the four quadrants were separately measured. A similar probe test (probe test II) was performed after two weeks from the probe test I.

All the tests were recorded by a video camera positioned right above the pool. A trace, total distance and speed of the swimming and the goal judge were analyzed by using a computer-operated system (TimeMWM; O'Hara & Co., Tokyo, Japan). Rate of the recording was 25 frames/sec.

Intracerebroventricular injection of steroids for Morris water maze test

A *Cyp7b1* KO male mouse was anesthetized by an intraperitoneal injection (20 μL/g body weight) of a mixture of ketamine (4.4 mg/mL; Daiichi Sankyo Propharma) and xylazine (0.44 mg/mL; Bayer Health Care) dissolved in bacteriostatic saline. The anaesthetized animal was placed in a stereotaxic frame as described above. A small hole was drilled in the skull, and a chronic

indwelling stainless-steel cannula (ALZET Brain Infusion Kit 1; DURECT Co.) was placed into the right lateral ventricle using the following coordinates relative to bregma: 0.22 mm posterior; 1.0 mm right lateral; 2.3 mm below the horizontal plane of bregma. The cannula was fixed to the skull with adhesive and dental cement, and the external part of the intracerebroventricular cannula was connected with polyethylene tube to an ALZET osmotic minipump with a infusion rate of 0.11 μL/h for four weeks (model 1004; DURECT Co.) placed subcutaneously on the back. Steroids were dissolved in an aCSF containing 1% DMSO. aCSF was prepared as described above. The concentration of 7α-OH-Preg (Steraloids Inc.) or 7α-OH-DHEA (Steraloids Inc.) solution was 910 ng/μL, and that of the mixed steroid solution was 455 ng/μL each of 7α-OH-Preg and 7α-OH-DHEA. The dose of steroids was chosen based on the previous study (Yau *et al.*, 2006). The steroid injection was made at a rate of 100 ng/h. All the mice were handled for at least one week before the surgery, housed individually after the surgery and allowed at least three days to recover.

3. Results

Expression profiles of genes responsible for neurosteroidogenesis

I examined mRNA expression profiles of genes responsible for biosynthesis of 7α-OH-Preg and 7α-OH-DHEA (Figure 1) in various brain regions of wild-type (WT) mice. The mRNAs encoding the enzymes required for the synthesis of 7α-OH-Preg and 7α-OH-DHEA were detected in all the brain regions I examined (Figure 2). Due to a day-night variation in production of 7α-OH-Preg in the brain of newt (Koyama *et al.*, 2009), quail (Tsutsui *et al.*, 2008) and chicken (Hatori *et al.*, 2011), I investigated the expression of mRNAs in the mouse brain regions prepared at two time points, zeitgeber time 6 (ZT6) and ZT18 (ZT0 is defined as the time of lights-on and ZT12 as the time of lights-off). The expression levels of *Cyp7b1*, a key enzyme for the production of both 7α-OH-Preg and 7α-OH-DHEA, were high in the hippocampal CA1 and dentate gyrus (DG) among the brain regions (Figure 2A). *Cyp7b1* mRNA showed day-night change with higher levels at ZT18 (nighttime) than at ZT6 (daytime) in the hippocampus (Figure 2A). I then examined mRNA expressions for *StAR* and *Cyp11a1,* both of which are responsible for production of pregnenolone, a common precursor of neurosteroids (Figure 1). In several brain regions, the mRNA expression levels of *StAR* (Figure 2B) and *Cyp11a1* (Figure 2C) were higher at ZT18 than at ZT6, suggesting daily changes in the amounts of neurosteroids. mRNA expression of *Cyp17a1* responsible for biosynthesis of DHEA (Payne *et al.*, 2004) was detected in the mouse brain, relatively high in the diencephalon, cerebellum, medulla and pineal gland, with no significant day-night change in any brain regions (Figure 2D).

Detection of 7α-OH-Preg and 7α-OH-DHEA in the hippocampus

To the best of my knowledge, neither 7α-OH-Preg nor 7α-OH-DHEA has been detected in the rodent brain. In the present study, I employed ultra-performance liquid chromatography coupled with electrospray-tandem mass spectrometry (UPLC/ESI-MS/MS) for detecting 7α-OH-Preg and 7α-OH-DHEA.

I modified the steroid extraction method of the previous gas chromatography/mass spectrometric analysis (Matsunaga *et al.*, 2004) for 7α-OH-Preg and 7α-OH-DHEA. Optimal purification condition for 7α-OH-Preg and 7α-OH-DHEA was determined by using a solid-phase extraction (SPE) column. The standard mixture (7α-OH-Preg, 7α-OH-DHEA, pregnenolone, and DHEA) was loaded on the column and eluted step-wisely with different concentrations of methanol (MeOH) and each fraction was analyzed using HPLC with UV detection at 200 nm. 7α-OH-Preg and 7α-OH-DHEA were not eluted by <50% MeOH aq. but eluted by 75% MeOH aq. Then, I tried to load the mixture sample in 37.5% MeOH aq. and elute it by 75% MeOH aq., and confirmed that the target steroids were extracted in the new condition (Figure 3).

Because 3β-hydroxylated steroids were preferably detected as multiply dehydrated forms in positive-ion mode (Mikšík *et al.*, 2004), which led to production of diverse ions with lower intensities, I used negative-ion mode for detecting $[M-H]^-$ ion (Figure 4). Furthermore, the selectivity and sensitivity in the MS detection were enhanced by using multiple reaction monitoring (MRM) mode. First, on MRM mode, a precursor ion with a specific *m/z* is selected and transmitted. This precursor ion is fragmented, and only a unique product ion is detected. Because of two stages of mass selection, target compounds are analyzed with high sensitivity. Therein, I set three major product ions (= MRM transitions) for each of 7α-OH-Preg and 7α-OH-DHEA based on MS/MS spectra

of each standard sample (Figure 5, Table 1). They were eluted at 8.3 min and 7.7 min respectively, and each gave specific peak intensities for the three MRM transitions (Figure 6A, B). For compound identification, the peaks at each MRM transition should have the same retention time as those of the standards, with their relative intensities parallel with those of the standards. As the result, 7α-OH-Preg (Figure 6C) and 7α-OH-DHEA (Figure 6D) were identified in the mouse hippocampal extract prepared at ZT1-3.

Validation of *Cyp7b1* KO mouse model

In the present study, I used *Cyp7b1* KO mice (Li-Hawkins *et al.*, 2000) to examine physiological roles of the 7α-hydroxylated steroids. It has been reported that CYP7B1 is the only enzyme that catalyzes 7α-hydroxylation of steroids in the mouse brain (Rose *et al.*, 1997, 2001). In contrast to CYP7B1 hydroxylating 7α-position of pregnenolone, CYP7A1 is known to hydroxylate 7α-position of cholesterol in the liver for biosynthesis of bile acids, and this reaction is catalyzed by liver CYP7B1 in case of *Cyp7a1* deficiency (Ishibashi *et al.*, 1996; Schwarz *et al.*, 1996). Therefore, I cannot exclude the possibility that CYP7A1 might provide a salvage pathway producing 7α-OH-Preg and/or 7α-OH-DHEA if *Cyp7b1* deficiency would cause ectopic expression of CYP7A1 in the brain. This possibility was tested by examining mRNA expression of *Cyp7a1* in the hippocampus and the pineal gland of *Cyp7b1* KO mice. RT-qPCR analysis demonstrated no detectable expression of *Cyp7a1* mRNA at any time of day in *Cyp7b1* KO mice (and also in WT mice) under the condition that *Cyp7a1* mRNA was detected in the WT liver (Figure 7). And, no significant amount of 7α-OH-Preg and 7α-OH-DHEA was detected in the hippocampal extracts of *Cyp7b1* KO mice.

Daily locomotor activity of *Cyp7b1* KO mice

It has been reported that 7α-OH-Preg upregulates locomotor activities in newt (Matsunaga *et al.*, 2004), quail (Tsutsui *et al.*, 2008) and chicken (Hatori *et al.*, 2011), whereas, in mammals, 7α-OH-Preg or CYP7B1 is suggested to be associated with memory performance and mental states (and disorders) (Yau *et al.*, 2003, 2006; Stiles *et al.*, 2009). I investigated spontaneous locomotor activities of *Cyp7b1* KO mice maintained in a 12 hr light/dark cycle (LD). No significant difference was observed in locomotor activity levels during the nighttime between *Cyp7b1* KO and the littermate WT mice (Figure 8). A small increase in the activity was detected at ZT8-9 and ZT10-11 in *Cyp7b1* KO mice (Figure 8A), but the total activity levels in the afternoon (ZT6-12) were indistinguishable between the two genotypes (Figure 8B). In constant darkness (DD), there was no significant difference in the activity levels except a slightly higher activity of *Cyp7b1* KO mice at circadian time (CT) 9-10 (the time points of the onsets of mice activity were defined as CT12) (Figure 8C, D). Consistently, daily oscillations in the mRNA expression levels of albumin D-site binding protein (*Dbp*), one of the clock-controlled output genes, and arylalkylamine *N*-acetyltransferase (*Aanat*), one of the enzymes for diurnal melatonin synthesis expressed only in the eye and the pineal gland, were not affected by *Cyp7b1* deficiency in the hippocampus and the pineal gland (Figure 9). I also examined circadian rhythmicity of locomotor activity in the mutant mice under constant darkness (Figure 10A) and found that *Cyp7b1* deficiency caused no detectable change in the free running period (Figure 10B) and the phase shift (delay or advance) by a light pulse given at CT14 or 22, respectively (Figure 10C).

Emotional phenotypes of *Cyp7b1* KO mice

Previous reports suggest relationships between *Cyp7b1* and neurological diseases (Yau *et al.*, 2003; Stiles *et al.*, 2009). Therefore, I investigated the effect of 7α-OH-Preg on emotional phenotypes of mice. Using *Cyp7b1* KO and littermate WT mice, I performed elevated plus maze (EPM) test, open field (OF) test, and forced swimming (FS) test in this order. EPM and OF tests are experiments for the estimation of anxiety-like behaviors of mice, and FS test is that for depression-like behavior. Because I revealed that the expression of mRNA of *Cyp7b1* showed diurnal variation in the mice pineal gland and hippocampus (Figure 2), each test was conducted at two different time points during the daytime, ZT1 (dawn) and ZT11.5 (dusk).

In EPM test (Figure 11A, B) and OF test (Figure 11C), there was no significant difference between genotypes or between the time points of the experiments.

In FS test, immobility time is regarded as a behavioral measure of depression in the behavioral despair model (Porsolt *et al.*, 1977); the more depression-like state a mouse becomes, the longer immobility time it marks, because it should give up escaping from the deep and high-wall pool. WT mice showed significantly shorter immobility time at ZT1 than at ZT11.5 (Figure 12A). On the other hand, *Cyp7b1* KO mice did not exhibit such time-dependent variations in FS test, and its immobility time at ZT1 was longer than that of WT mice. This result indicated that, in WT mice, diurnal expression of CYP7B1 created diurnal variation in the depression-like behavior, which is lowered early in the morning. I tried to rescue the deficit of CYP7B1 by treatment of 7α-OH-Preg and/or 7α-OH-DHEA. However, there was no significant change in depression-like behavior after the intracerebroventricular injection of 7α-OH-Preg and/or 7α-OH-DHEA (Figure 12B, C).

Impaired spatial memory in *Cyp7b1* KO mice and its rescue by 7α-hydroxylated steroids

It was previously shown that impaired spatial memory in aged rats was ameliorated by central administration of 7α-OH-Preg (Yau *et al.*, 2006). Here I investigated spatial memory in *Cyp7b1* KO and the littermate WT mice by performing the Morris water maze task (Figure 13). The male mice were divided into four groups (for experiments on KO and WT each at ZT1 and ZT11.5) and trained for consecutive five days with four trials per day. In the training trials, the escape latency (time duration) to reach a hidden platform (Figure 14A) and the distance (Figure 14B) were both decreased on a daily basis. I found no significant difference in the learning curves between *Cyp7b1* KO and WT mice at each time point and between ZT1 and ZT11.5 in each genotype (Figure 14A, B). On the next day after five-day training trials, each animal was subjected to a probe test (probe test I for recent spatial memory), in which the hidden platform was removed and a time spent in exploring the platform (goal) quadrant, the opposite quadrant (O), and the side quadrants (S, an average of right and left quadrants) was measured (termed stay time) (Figure 13). In every group, the stay time ratio in the goal quadrant (G) was significantly higher than the chance level (25%) (Figure 14C). The stay time ratios in the goal quadrant (G) were similar among the four groups (Figure 14D). Thus, *Cyp7b1* KO and WT mice form recent spatial memory with efficacy indistinguishable from each other.

Two weeks after the probe test I, the mice in the four groups were subjected to the probe test again (probe test II for remote spatial memory). I found that WT mice explored the goal quadrant (G) significantly longer than the chance level at both ZT1 and ZT11.5 (Figure 14E). Here I should emphasize that the stay time ratio in the goal quadrant (G) at ZT1 was significantly higher than that at ZT11.5 (Figure 14F), indicating a daily variation in remote spatial memory in WT mice.

On the other hand, *Cyp7b1* KO mice that trained at ZT1 explored the goal quadrant (G) apparently longer than the other quadrants (O and S), but their selectivity to the goal quadrant (G) was low and the stay time ratio to the goal quadrant (G) was not significantly higher than the chance level (25%) (Figure 14E). A comparison between the two genotypes at ZT1 demonstrated that spatial memory retention was impaired by *Cyp7b1* deficiency (Figure 14F), whereas no significant difference in remote spatial memory was detected at ZT11.5 between the two genotypes. In these experiments, the swimming distance and the swimming speed in both of the probe tests were comparable among the four groups (Figure 15A-D).

The phenotype in remote memory of *Cyp7b1* deficiency observed only at ZT1 (Figure 14F) raised the possibility that 7α-OH-Preg and/or 7α-OH-DHEA may be responsible for remote memory in the morning (ZT1). To test this idea, *Cyp7b1* KO mice were divided into four groups administered artificial cerebrospinal fluid containing 1% DMSO (vehicle), 910 ng/μL 7α-OH-Preg (7αP), 910 ng/μL 7α-OH-DHEA (7αD), and 455 ng/μL each of 7α-OH-Preg plus 7α-OH-DHEA (7αP+7αD) intracerebroventricularly for four weeks by using osmotic minipump (0.11 μL/h; 100 ng/h). Three to five days after the infusion onset, mice were subjected to a series of the Morris water maze tasks at ZT1 (Figure 16). In the training trials and the subsequent probe test I for recent spatial memory, I found no significant difference among the four groups in not only the learning curves of the escape latency (Figure 16A) and the distance (Figure 16B) but also the stay time ratios in the goal quadrant (G) (Figure 16C, D). In the probe test II performed two weeks later from the probe test I, the stay time ratio to the goal quadrant (G) was comparable to the chance level in vehicle-infused *Cyp7b1* KO mice (Figure 16E; vehicle), which is consistent with the phenotype of *Cyp7b1* KO mice observed at ZT1 (Figure 14E; KO, ZT1). On the other hand, in *Cyp7b1* KO mice infused with 7α-OH-Preg (7αP) or 7α-OH-DHEA (7αD),

their stay time ratios to the goal quadrant (G) were significantly higher than the chance level (Figure 16E; 7αP and 7αD). Most strikingly, infusion of a mixture of 7α-OH-Preg and 7α-OH-DHEA (7αP+7αD) into *Cyp7b1* KO mice remarkably enhanced the stay time ratio to the goal quadrant (Figure 16E, F; 7αP+7αD). Intracerebroventricular infusion did not affect the swimming ability of mice (Figure 15E-H). It is noteworthy that *Cyp7b1* KO mice infused with a mixture of 7α-OH-Preg and 7α-OH-DHEA showed extremely higher remote memory performance than the single-infused *Cyp7b1* KO mice, although the total amounts of 7α-hydroxylated steroids (910 ng/μL) are equivalent among the three groups (Figure 16F).

4. Discussion

In the Morris water maze test, I found no detectable difference in recent spatial memory between *Cyp7b1* KO and WT mice (Figure 14C, D). On the other hand, remote spatial memory performance at ZT1 was impaired by *Cyp7b1* deficiency (Figure 14E, F). These results indicate that CYP7B1 should play a key role in a pathway that is specific to remote spatial memory but not to recent memory, probably through the actions of 7α-OH-Preg and 7α-OH-DHEA. Remote spatial memory formation is related to neuronal structural changes such as dendritic spine growth in the hippocampus (Leuner *et al*., 2003; Restivo *et al*., 2009; Mahmmoud *et al*., 2015). The spine density represents the number of hippocampal excitatory synapses (Moser *et al*., 1994; Leuner *et al*., 2003) and it was reported that the density in hippocampal neurons increased after spatial memory tasks (Moser *et al*., 1994; Eilam-Stock *et al*., 2012). The dendritic spines are balanced dynamically between additions and eliminations (Berry *et al*., 2017). I think that 7α-OH-Preg and 7α-OH-DHEA may be associated with regulation of spine dynamics in the hippocampus and bolster remote memory.

Remote spatial memory performance impaired in *Cyp7b1* KO mice was markedly ameliorated by intracerebroventricular infusion of a mixture of 7α-OH-Preg and 7α-OH-DHEA (455 ng/μL each) into the brain (Figure 16E, F) to a level similar to that of WT (Figure 14F; ZT1). I should emphasize that the co-injection of these neurosteroids was more effective than the single injection, although the concentrations of the singly administered steroids (910 ng/μL) were the same with the total concentration of the mixture (Figure 16F). I conclude that 7α-OH-Preg and 7α-OH-DHEA play a synergistic role in the long-term maintenance of spatial memory. It is possible to speculate that 7α-OH-Preg and 7α-OH-DHEA may have their own targets of action for the retention of

spatial memory. The targets of 7α-OH-Preg and 7α-OH-DHEA should be identified for the understanding of molecular mechanisms underlying the maintenance of remote spatial memory.

In the previous literature, 7α-OH-Preg has been identified as the trimethylsilyl ether derivative in the newt brain extract (Matsunaga *et al.*, 2004) and later in the brain extracts of quail (Tsutsui *et al.*, 2008) and chicken (Hatori *et al.*, 2011) by gas chromatography/mass spectrometric analysis. In the present study, I employed UPLC/ESI-MS/MS analysis in a negative-ion mode and detected 7α-OH-Preg in the mouse hippocampal extract without any derivatization (Figure 6). To my knowledge, this is the first demonstration of 7α-OH-Preg in the brain of mammalian species. On the other hand, 7α-OH-DHEA was previously detected in the ventricular cerebrospinal fluid of human (Stárka *et al.*, 2009) but not in the rodent brain.

Steroids can be converted to various forms and some reactions are reversible (Kihel *et al.*, 2012; Weng *et al.*, 2016). Therefore, it is very difficult to determine which steroid is the physiologically active molecule in biological functions. Although further conversion is not reported about 7α-OH-Preg and 7α-OH-DHEA, there is a possibility that 7α-OH-Preg may be hydroxylated by CYP17A1 to 7α-OH-DHEA in the mouse brain and only 7α-OH-DHEA might be effective for remote spatial memory, or *vice versa*. However, the result of Morris water maze test of co-injected *Cyp7b1* KO mice (Figure 16F) suggests that 7α-OH-Preg and 7α-OH-DHEA may have each own role. Therefore, I think that both 7α-OH-Preg and 7α-OH-DHEA may have their own receptors and active roles in remote spatial memory.

Cyp7b1 KO mice exhibited more depressive (Figure 12A) and lower retention remote memory (Figure 14E, F) than WT mice at ZT1. Intracerebroventricular injection of 7α-OH-Preg and 7α-OH-DHEA seems to affect remote spatial memory (Figure 16E, F) but not depression-like behavior (Figure 12B, C). CYP7B1 can also convert other steroids (Rose *et al.*, 1997). Therefore, there remains a possibility that the decline of depression-like behavior in *Cyp7b1* KO mice might be triggered by other biological functions of CYP7B1, such as excretion or metabolism of various other steroid hormones (Weihua *et al.*, 2002). For example, corticosterone is secreted from adrenal glands around the time of activity onset in mice (Sollars *et al.*, 2014) and can be hydroxylated to a metabolite by CYP7B1. Since corticosterone exposure induces depression-like behavior (Murata *et al.*, 2018), *Cyp7b1* KO mice might be considered to become more depressive than WT mice because of high-level corticosterone. On the other hand, WT mice should be able to metabolize corticosterone by CYP7B1 during the dark period and demonstrate lower depression-like behavior at ZT1 than at ZT11.5. There may be other steroids contributing to depression-like behavior and its diurnal change. The loss of steroid 7α-hydroxylation ability may disrupt the diurnal regulation of depression-like behavior in *Cyp7b1* KO mice.

WT mice showed a time-dependent difference in depression-like behavior and memory retention: less depressive in forced swimming test (Figure 12A) and higher retention of remote spatial memory in Morris water maze test (Figure 14F) at ZT1 than at ZT11.5. Since most of predators of mice are crepuscular animals, *e.g.* feral cats (Izawa *et al.*, 1983) or coyotes (Lashley *et al.*, 2018), it is quite important for mice to keep their courage and memory retention at the beginning and at the end of the daytime.

Up to the present, 7α-OH-Preg was reported as a neurosteroid that increases locomotor activity in newt, quail and chicken, (Matsunaga *et al.*, 2004; Tsutsui *et al.*, 2008; Koyama *et al.*, 2009; Hatori *et al.*, 2011). In newt, 7α-OH-Preg might induce dopamine release and consequently increase locomotor activity through dopamine D_2 receptor (Matsunaga *et al.*, 2004). 7α-OH-Preg-deficient *Cyp7b1* KO mice, however, have no phenotype on the spontaneous locomotor activity, its daily pattern and the circadian profile (Figure 8, 10). Similarly, the swimming distance and the swimming speed in the Morris water maze task were unaffected not only by *Cyp7b1* deficiency but also by infusion of 7α-hydroxylated steroids into the brain of the mutant mouse (Figure 15). Thus, it is concluded 7α-Hydroxylated steroids do not play a role in the regulation of locomotor activity, at least in mice.

According to previous studies in newt and quail (Tsutsui *et al.*, 2008, 2010), the production of 7α-OH-Preg is related to melatonin secretion. Melatonin level becomes higher during the dark phase (Klein *et al.*, 2007). Interestingly, response to melatonin is different in each animal. In diurnal quail, locomotor activity decreases during the dark phase and the production of 7α-OH-Preg is inhibited by melatonin. On the other hand, in nocturnal newt, locomotor activity increases during the dark phase, and the production of 7α-OH-Preg is promoted by melatonin (Tsutsui *et al.*, 2010). Since C57BL/6 mice have no ability to produce melatonin, the simplified behavior and function of 7α-OH-Preg should be observed in this strain without the effect of melatonin.

I found that mRNA expression of *Cyp7b1* was low in daytime (ZT6) and high in nighttime (ZT18) in the hippocampus (Figure 2A), and therefore, hippocampal 7α-hydroxylated steroids may be produced with a

daily variation. Such a daily change in levels of 7α-hydroxylated steroids may cause the dawn-dusk difference in mouse behavioral tests for remote spatial memory (Figure 14F). In contrast, pineal mRNA level of *Cyp7b1* was higher in daytime (ZT6) than in nighttime (ZT18), a profile different from that in the hippocampus (Figure 2A). While 7α-OH-Preg synthesized diurnally in the hippocampus should be responsible for remote spatial memory within the local region, 7α-OH-Preg secreted from the mouse pineal gland may play a different role in other regions by paracrine or endocrine effect. I speculate that 7α-OH-Preg may be secreted diurnally in mice as well as in newt (Koyama *et al.*, 2009) and birds (Tsutsui *et al.*, 2008; Hatori *et al.*, 2011), and the secretion may induce diurnal variation of remote spatial memory in mice. However, since receptors or signaling pathways of 7α-OH-Preg and 7α-OH-DHEA are not unclear, I should point out that a possibility still remains that their receptors may be expressed diurnally and generate diurnal variation of mouse behaviors while these steroids may be secreted constantly all day. It is a future work to clarify diurnal variations of steroids themselves using the newly developed UPLC/ESI-MS/MS analysis.

5. Conclusion

In conclusion, RT-qPCR analysis demonstrated wide expression of *Cyp7b1* mRNA in the mouse brain, especially relatively high-level expression and the day-night change of the level in the hippocampus. By using ultra performance liquid chromatography coupled tandem mass spectrometry, I identified 7α-OH-Preg and 7α-OH-DHEA in the mouse hippocampal extract. *Cyp7b1*-deficiency in mice impaired long-term maintenance of hippocampus-dependent spatial memory, which was significantly ameliorated by simultaneous intracerebroventricular infusion of 7α-OH-Preg and 7α-OH-DHEA than their single infusion. Based on these results, I conclude that CYP7B1 plays a key role in remote spatial memory, most probably through the cooperative action of the 7α-hydroxylated neurosteroids.

6. Reference

Akwa Y, Morfin RF, Robel P, Baulieu E-E (1992) Neurosteroid metabolism. 7α-Hydroxylation of dehydroepiandrosterone and pregnenolone by rat brain microsomes. *Biochem J* 288:959-964.

Baulieu ÉÉ (2000) 'New' active steroids and an unforeseen mechanism of action. *C R Acad Sci III* 323:513–518.

Berry KP, Nedivi E (2017) Spine Dynamics: Are They All the Same? *Neuron* 96:43-55.

Corpéchot C, Robel P, Axelsont M, Sjövall J, Baulieu E-E (1981) Characterization and measurement of dehydroepiandrosterone sulfate in rat brain. *Proc Natl Acad Sci USA* 78:4704-4707.

Eilam-Stock T, Serrano P, Frankfurt M, Luine V (2012) Bisphenol-A impairs memory and reduces dendritic spine density in adult male rats. *Behav Neurosci* :175-185.

Hatori M, Hirota T, Iitsuka M, Kurabayashi N, Haraguchi S, Kokame K, Sato R, Nakai A, Miyata T, Tsutsui K, Fukada Y (2011) Light-dependent and circadian clock-regulated activation of sterol regulatory element-binding protein, X-box-binding protein 1, and heat shock factor pathways. *Proc Natl Acad Sci USA* 108:4864-4869.

Ishibashi S, Schwarz M, Frykman PK, Herz J, Russell DW (1996) Disruption of cholesterol 7α-hydroxylase gene in mice. I. Postnatal lethality reversed by bile acid and vitamin supplementation. *J Biol Chem* 271:18017-18023.

Izawa M. (1983) Daily activities of the feral cat *Felis catus* Linn. *J Mammalogical Soc Japan* 9:219-228.

Kihel LE (2012) Oxidative metabolism of dehydroepiandrosterone (DHEA) and biologically active oxygenated metabolites of DHEA and epiandrosterone (EpiA)-recent reports. *Steroids* 77:10-26.

Klein DC (2007) Arylalkylamine N-Acetyltransferase: "the Timezyme." *J Biol Chem* 282:4233-4237.

Koyama T, Haraguchi S, Vaudry H, Tsutsui K (2009) Diurnal changes in the synthesis of the neurosteroid 7a-hydroxypregnenolone stimulating locomotor activity in newts. *Ann N Y Acad Sci* 1163:444-447.

Lashley MA, Cove M V, Chitwood MC, Penido G, Gardner B, DePerno CS *et al*. (2018) Estimating wildlife activity curves : comparison of methods and sample size. *Sci Rep* 8:4173.

Leuner B, Falduto J, Shors TJ (2003) Associative memory formation increases the observation of dendritic spines in the hippocampus. *J Neurosci* 23:659-665.

Li-Hawkins J, Lund EG, Turley SD, Russell DW (2000) Disruption of the oxysterol 7α-hydroxylase gene in mice. *J Biol Chem* 275:16536-16542.

Mahmmoud RR, Sase S, Aher YD, Sase A, Gröger M, Mokhtar M, Höger H, Lubec G. (2015) Spatial and working memory is linked to spine density and mushroom spines. *PLoS One* 10:e0139739.

Matsunaga M, Ukena K, Baulieu E-E, Tsutsui K (2004) 7a-Hydroxypregnenolone acts as a neuronal activator to stimulate locomotor activity of breeding newts by means of the dopaminergic system. *Proc Natl Acad Sci USA* 101:17282-17287.

Mikšík I, Mikulíková K, Pácha J, Kučka M, Deyl Z (2004) Application of liquid chromatography-electrospray ionization mass spectrometry for study of steroid-converting enzymes. *J Chromatogr B* 800:145-153.

Morfin R, Courchay G (1994) Pregnenolone and dehydroepiandrosterone as precursors of native 7-hydroxylated metabolites which increase the immune response in mice. *J Steroid Biochem Mol Biol* 50:91-100.

Moser MB, Trommald M, Andersen P (1994) An increase in dendritic spine density on hippocampal CA1 pyramidal cells following spatial learning in adult rats suggests the formation of new synapses. *Proc Natl Acad Sci USA* 91:12673-12675.

Omoto Y, Lathe R, Warner M, Gustafsson J-Å (2005) Early onset of puberty and early ovarian failure in CYP7B1 knockout mice. *Proc Natl Acad Sci USA* 102:2814-2819.

Oyola MG, Zuloaga DG, Carbone D, Malysz AM, Acevedo-Rodriguez A, Handa RJ, Mani SK (2015) CYP7B1 enzyme deletion impairs reproductive behaviors in male mice. *Endocrinology* 156:2150-2161.

Payne AH, Hales DB (2004) Overview of steroidogenic enzymes in the pathway from cholesterol to active steroid hormones. *Endocr Rev* 25:947-970.

Porsolt RD, LePichon M, Jalfre M. (1977) Depression: a new animal model sensitive to antidepressant treatments. *Nature* 266:730-732.

Pringle AK, Schmidt W, Deans JK, Wulfert E, Reymann KG, Sundstrom LE (2003) 7-Hydroxylated epiandrosterone (7-OH-EPIA) reduces ischaemia-induced neuronal damage both *in vivo* and *in vitro*. *Eur J Neurosci* 18:117-124.

Restivo L, Vetere G, Bontempi B, Ammassari-Teule M (2009) The formation of recent and remote memory is associated with time-dependent formation of dendritic spines in the hippocampus and anterior cingulate cortex. *J Neurosci* 29:8206-8214.

Rose KA, Stapleton G, Dott K, Kieny MP, Best R, Schwarz M, Russell DW, Björkhem I, Seckl J, Lathe R (1997) Cyp7b, a novel brain cytochrome P450, catalyzes the synthesis of neurosteroids 7a-hydroxy dehydroepiandrosterone and 7a-hydroxy pregnenolone. *Proc Natl Acad Sci USA* 94:4925-4930.

Rose K, Allan A, Gauldie S, Stapleton G, Dobbie L, Dott K, Martin C, Wang L, Hedlund E, Seckl JR, Gustafsson J-Å, Lathe R (2001) Neurosteroid hydroxylase CYP7B: Vivid reporter activity in dentate gyrus of gene-targeted mice and abolition of a widespread pathway of steroid and oxysterol hydroxylation. *J Biol Chem* 276:23937-23944.

Schwarz M, Lund EG, Setchell KDR, Kayden HJ, Zerwekh JE, Björkhem I, Herz J, Russell DW (1996) Disruption of cholesterol 7α-hydroxylase gene in mice. II. Bile acid deficiency is overcome by induction of oxysterol 7α-hydroxylase. *J Biol Chem* 271:18024-18031.

Stárka L, Hill M, Kancheva R, Novak Z, Chrastina J, Pohanka M, Morfin R (2009) 7-Hydroxylated derivatives of dehydroepiandrosterone in the human ventricular cerebrospinal fluid. *Neuroendocrinol Lett* 30:368-372.

Stiles AR, McDonald JG, Bauman DR, Russell DW (2009) CYP7B1: one cytochrome P450, two human genetic diseases, and multiple physiological functions. *J Biol Chem* 284:28485-28489.

Tsutsui K, Inoue K, Miyabara H, Suzuki S, Ogura Y, Haraguchi S (2008) 7a-Hydroxypregnenolone mediates melatonin action underlying diurnal locomotor rhythms. *J Neurosci* 28:2158-2167.

Tsutsui K, Haraguchi S, Matsunaga M, Inoue K, Vaudry H (2010) 7A-Hydroxypregnenolone, a New Key Regulator of Locomotor Activity of Vertebrates: Identification, Mode of Action, and Functional Significance. *Front Endocrinol* 1:9.

Tsutsui K, Haraguchi S, Fukada Y, Vaudry H (2013) Brain and pineal 7α-hydroxypregnenolone stimulating locomotor activity: Identification, mode of action and regulation of biosynthesis. *Front Neuroendocrinol* 34:179–189.

Tsutsui K, Haraguchi S, Vaudry H (2018) 7a-Hydroxypregnenolone regulating locomotor behavior identified in the brain and pineal gland across vertebrates. *Gen Comp Endocrinol* 265:97-105.

Weihua Z, Lathe R, Warner M, Gustafsson J-Å (2002) An endocrine pathway in the prostate, ERβ, AR, 5α-androstane-3β, 17β-diol, and CYP7B1, regulates prostate growth. *Proc Natl Acad Sci USA* 99:13589–13594.

Weng J-H, Chung B-C (2016) Nongenomic actions of neurosteroid pregnenolone and its metabolites. *Steroids* 111:54-59.

Wingfield JC, Wacker DW, Bentley GE, Tsutsui K (2018) Brain-derived steroids, behavior and endocrine conflicts across life history stages in birds: A perspective. *Front Endocrinol* 9:Article 270.

Yau JLW, Rasmuson S, Andrew R, Graham M, Noble J, Olsson T, Fuchs E, Lathe R, Seckl JR (2003) Dehydroepiandrosterone 7-hydroxylase CYP7B: predominant expression in primate hippocampus and reduced expression in Alzheimer's disease. *Neuroscience* 121:307-314.

Yau JLW, Noble J, Graham M, Seckl JR (2006) Central administration of a cytochrome P450-7B product 7α-hydroxypregnenolone improves spatial memory retention in cognitively impaired aged rats. *J Neurosci* 26:11034-11040.

7. Figures and Table

Table 1 Product ion species of 7α-OH-Preg and 7α-OH-DHEA employed in multiple reaction monitoring (MRM) analysis of UPLC/ESI-MS/MS (see Material and Methods in detail)

Compound Name	Retention Time (min)	Precursor Ion	MS1 Res	Product Ion	MS2 Res	Dwell	Fragmentor	Collision Energy	Cell Accelerator Voltage
7α-OH-Preg	8.310	331.2	Unit	315.2	Widest	50	170	25	4
	8.308			259.1				33	
	8.306			97.1				45	
7α-OH-DHEA	7.681	303.1	Unit	286.1	Widest	50	170	29	4
	7.680			245				33	
	7.679			97.1				41	

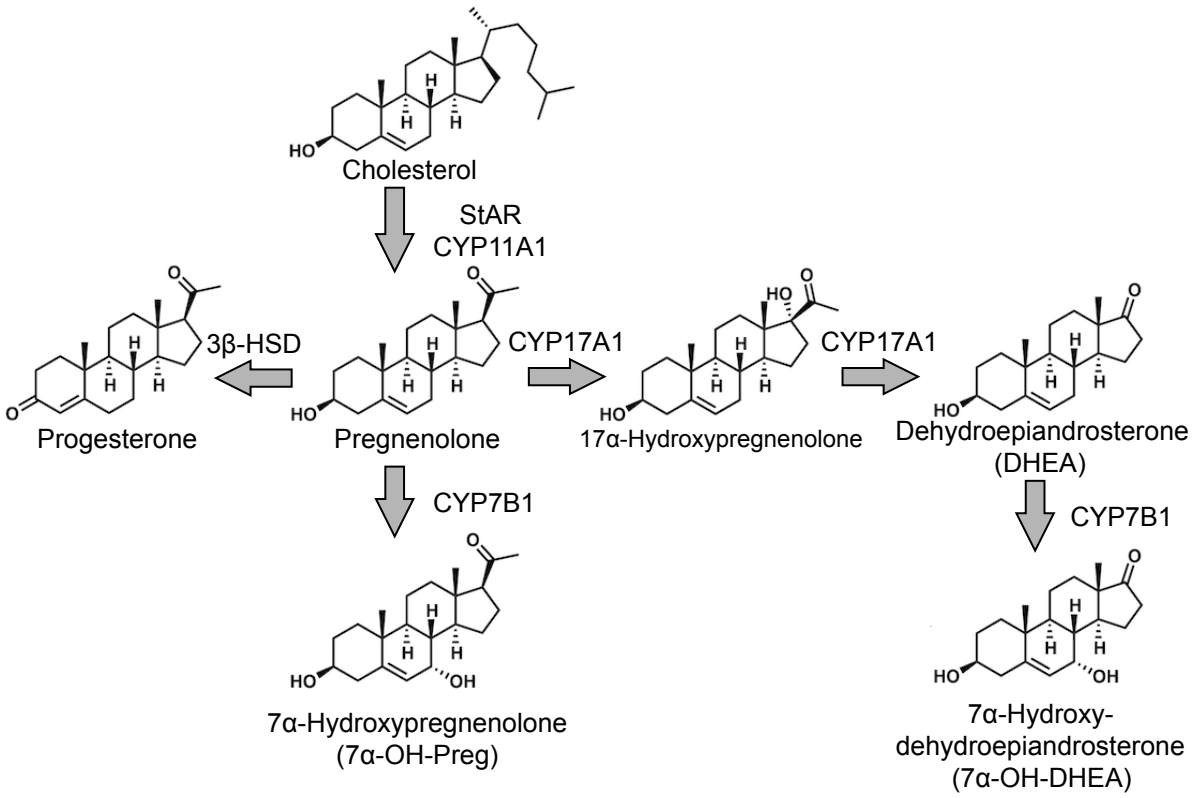

Figure 1 Biosynthetic pathways for 7α-hydroxylated neurosteroids

Steroidogenic acute regulatory protein (StAR) transfers cholesterol to the mitochondrial membrane, where CYP11A1 catalyzes conversion of cholesterol into pregnenolone. Pregnenolone is subsequently converted into various bioactive neurosteroids by hydroxylation and/or oxidation. As one of the conversion pathways, CYP7B1 catalyzes 7α-hydroxylation of pregnenolone for formation of 7α-OH-Preg. Alternatively, CYP17A1 catalyzes two-steps 17-oxydation of pregnenolone for formation of DHEA, which is then 7α-hydroxylated by CYP7B1 to form 7α-OH-DHEA.

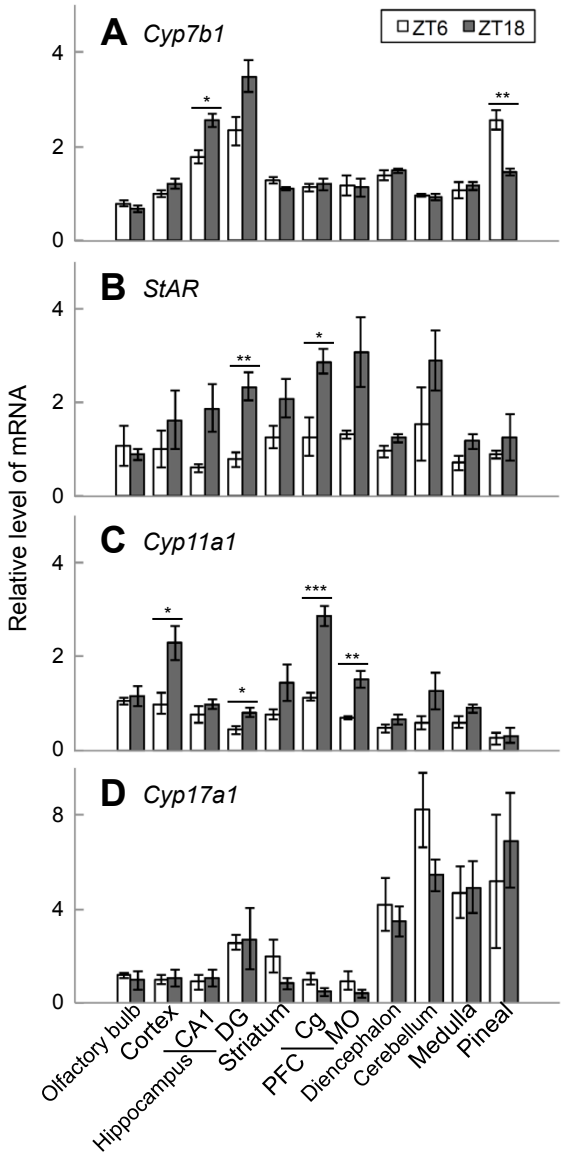

Figure 2 Expression profiles of genes responsible for 7α-OH-Preg and 7α-OH-DHEA biosynthesis in the mouse brain regions

The expression levels of mRNAs encoding (**A**) CYP7B1, (**B**) StAR, (**C**) CYP11A1, and (**D**) CYP17A1 were quantitated by RT-qPCR analysis of RNA samples prepared at ZT6 (daytime) and ZT18 (nighttime) from various mouse brain regions. CA1; hippocampal CA1 region, DG; dentate gyrus, Cg; cingulate cortex, MO; medial orbital cortex, PFC; prefrontal cortex. Data are normalized by mRNA levels of *Rps29*. The expression levels were presented as a ratio relative to that in cortex at ZT6. Values are shown as the mean ± SEM (n = 3-4). * $P < 0.05$, ** $P < 0.01$, *** $P < 0.001$ by Student's t test.

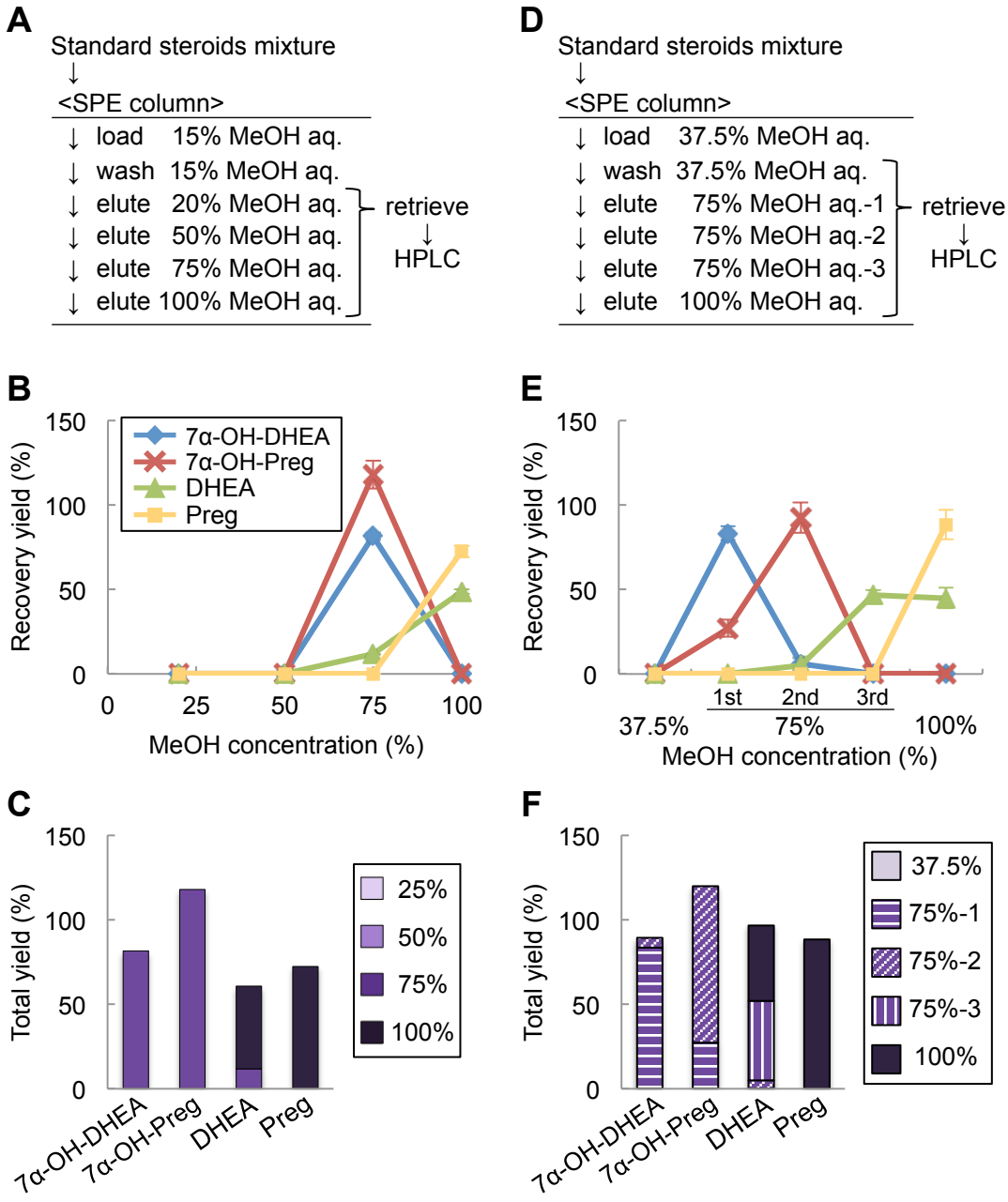

Figure 3 Optimization of purification condition with solid-phase extraction column

Mixed standard steroids of 7α-OH-DHEA, 7α-OH-Preg, dehydroepiandrosterone (DHEA), and pregnenolone (Preg) were loaded to a solid-phase extraction (SPE) column and eluted step-wisely for optimization of purification condition. Steroids in each fraction were analyzed by HPLC and detected by absorbance at 200 nm. First, examination of solvent concentration. (**A**) Experimental steps. (**B**) Overwritten elution profile. Recovery yields in each fraction were calculated based on the mixed standard steroids without passing SPE column. (**C**) Integrated yield of each steroid. From these results, the solvents for sample loading and steroid extraction were optimized. Next, examination of solvent volume. (**D**) Experimental steps. (**E**) Overwritten elution profile. (**F**) Integrated yield of each steroid.

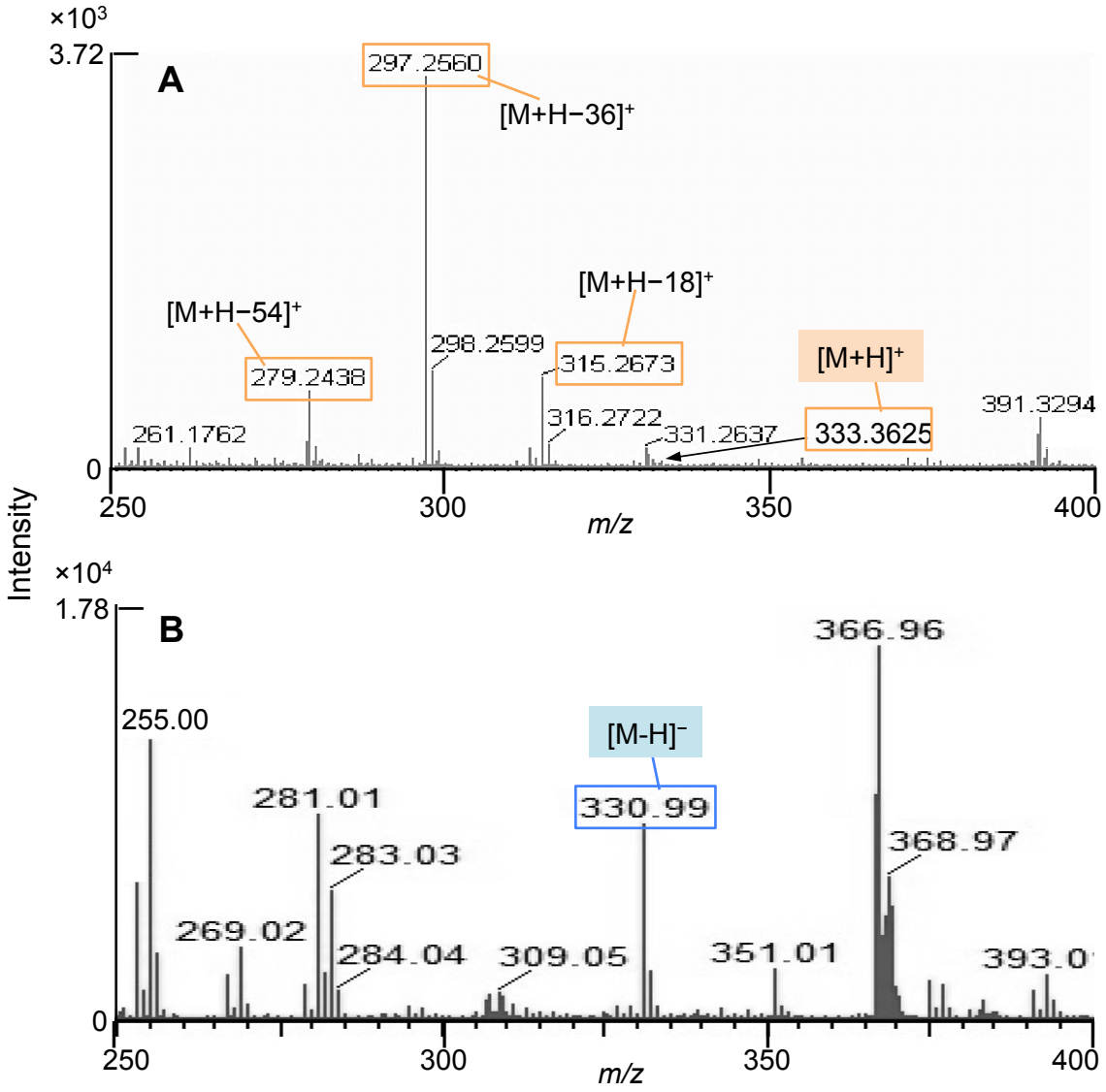

Figure 4 MS spectra of standard 7α-OH-Preg

(**A**) MS spectrum of standard 7α-OH-Preg was measured in positive ion mode. The intensity of the precursor ion ($M+H^+$) was low because multiple dehydration of the steroid hampered the detection. (**B**) In negative ion mode, the precursor ion ($M-H^-$) was detected with high intensity.

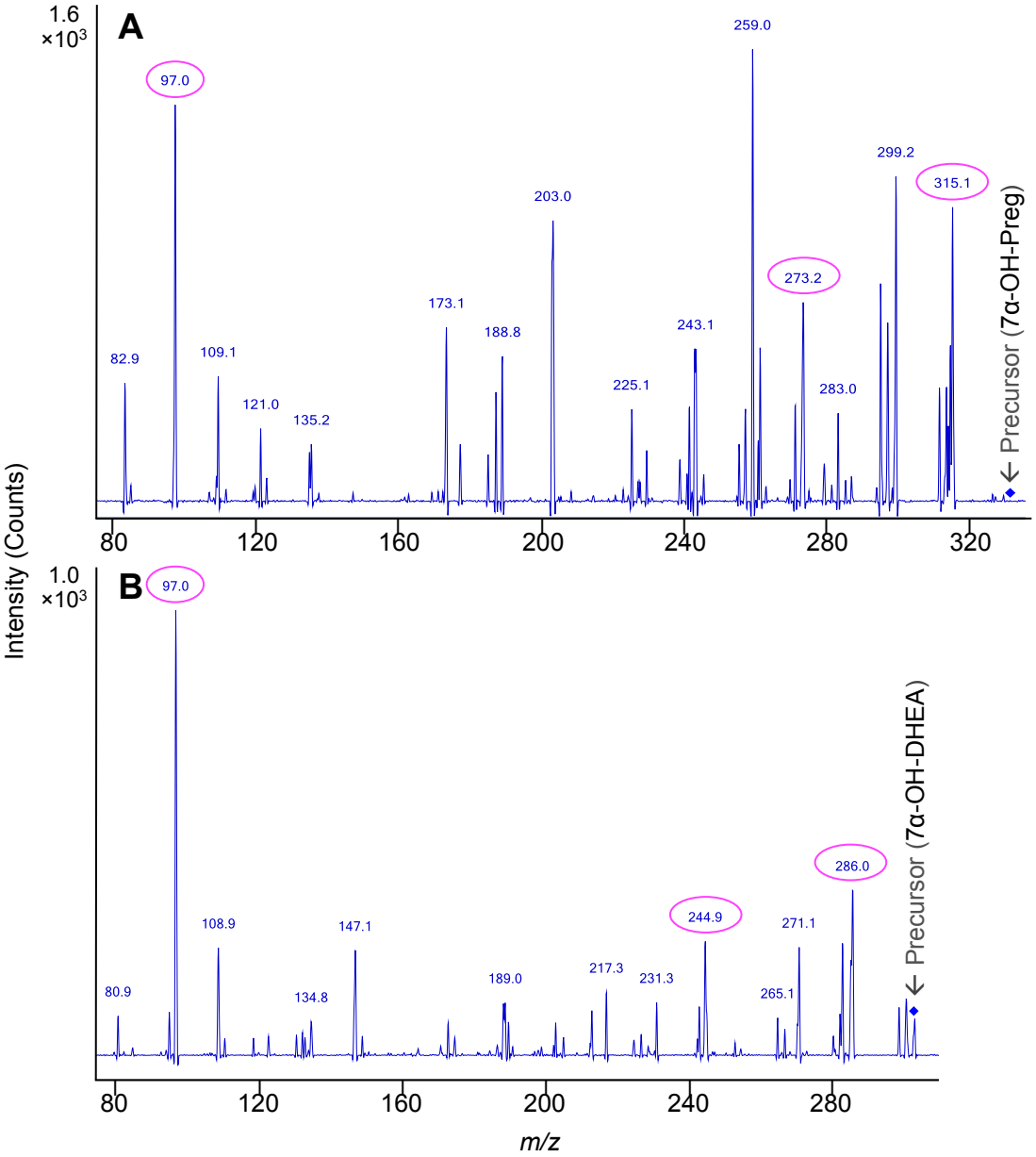

Figure 5 MS/MS spectra of standard 7α-hydroxylated steroids

In order to select MRM transitions for detecting target steroids, MS/MS spectra of standard steroids were measured by LC-MS/MS analysis. MS/MS spectra of standard solutions of 7α-OH-Preg at 8.3 min (**A**) and 7α-OH-DHEA at 7.7 min (**B**) (10 ng each). The selected product ions are marked by pink circle.

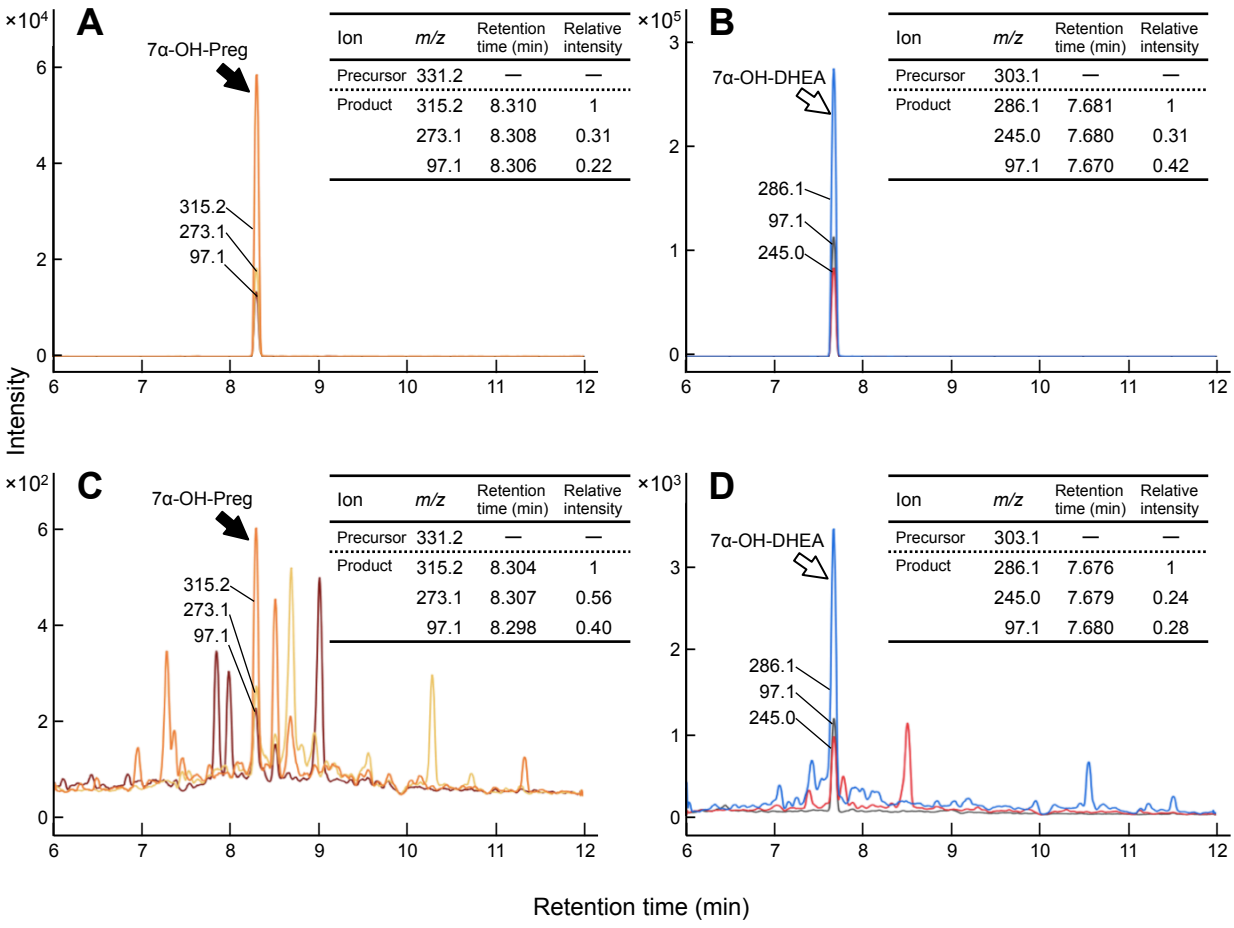

Figure 6 UPLC/ESI-MS/MS analysis of 7α-OH-Preg and 7α-OH-DHEA in the mouse hippocampal extract

MRM chromatograms of LC-MS/MS analysis of standard 7α-OH-Preg (**A**) and 7α-OH-DHEA (**B**) solutions (10 ng each) and the mouse hippocampal extract (**C**, **D**). (**A**, **C**) MRM transitions for detecting 7α-OH-Preg were 331.2->315.2 (orange), 331.2->273.1 (yellow) and 331.2->97.1 (claret). (**B**, **D**) MRM transitions for detecting 7α-OH-DHEA were 303.1->286.1 (blue), 303.1->245.0 (red) and 303.1->97.1 (gray). Relative peak intensities of these product ions are shown in the inset table.

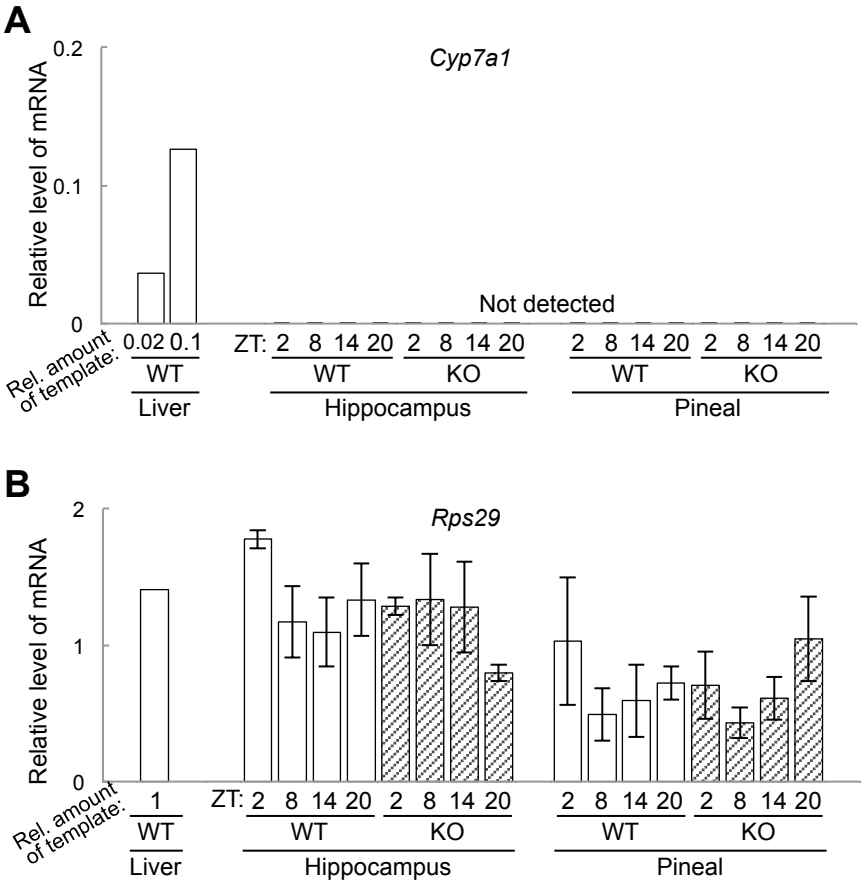

Figure 7 Investigation of mRNA expression of *Cyp7a1* in the brain of *Cyp7b1* KO and the littermate WT mice

The expression levels of mRNAs encoding (**A**) CYP7A1 and (**B**) RPS29 were quantitated by RT-qPCR analysis of RNA samples prepared at four time points from the mouse hippocampus, pineal gland, and liver. Pineal glands of three mice were pooled at each sample. Samples of standard curves were liver cDNA for *Cyp7a1* and hippocampal cDNA for *Rps29*. The lower detection limits of these assays were 0.005 for *Cyp7a1* and 0.01 for *Rps29*. Concerning the hippocampus and pineal gland, values are shown as the mean ± SEM (n = 3-4).

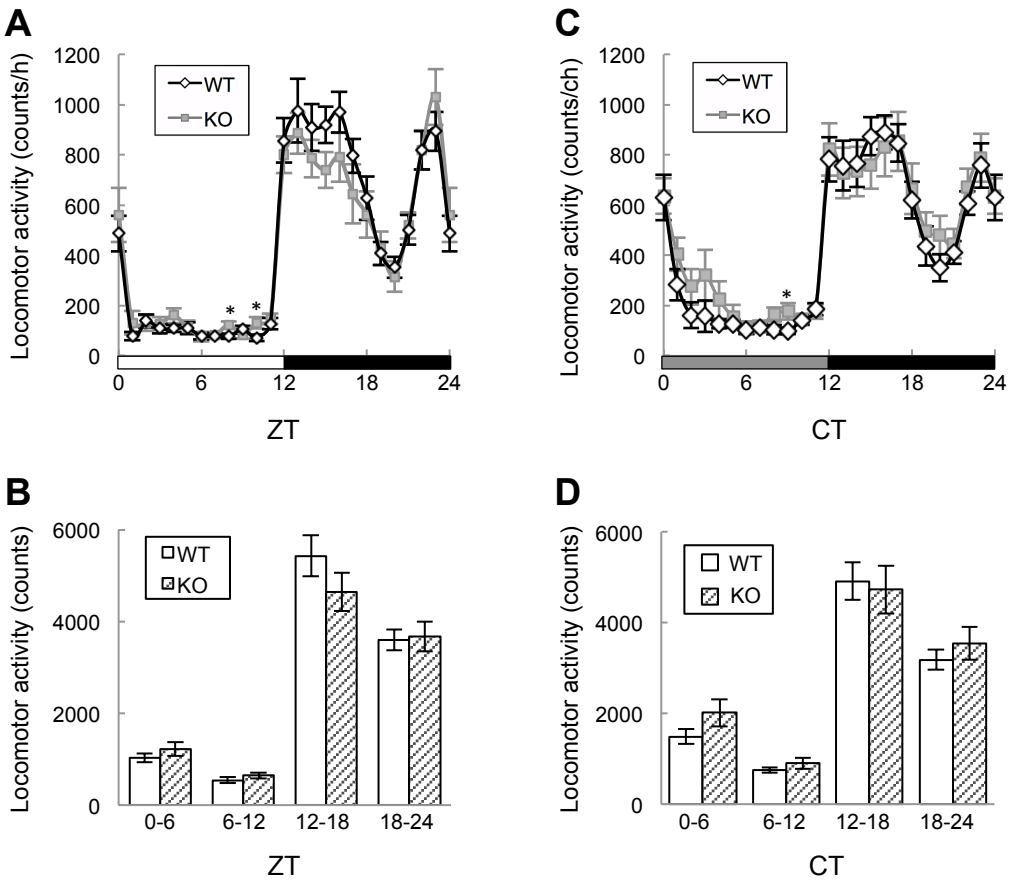

Figure 8 Spontaneous locomotor activities of *Cyp7b1* KO mice

Cyp7b1 KO and the littermate WT mice were entrained to 12 hr light/dark cycle (LD) and transferred to constant darkness (DD). Their free moving locomotor activities were monitored using infrared area sensors. (**A**) Averaged locomotor activities in LD (counts in one hour) were plotted against ZT. (**B**) Averaged locomotor activities in LD (counts in six hours) during the four time zones (ZT0-6, 6-12, 12-18, 18-24). (**C**) Averaged locomotor activities in DD (counts in one circadian hour) were plotted against CT. (**D**) Averaged locomotor activities in DD (counts in six circadian hours) during the four time zones (CT0-6, 6-12, 12-18, 18-24). Values are calculated from the averaged activities in 14 days for each mouse and shown as the mean ± SEM (WT, $n = 15$; KO, $n = 14$). * $P < 0.05$ by Student's t test.

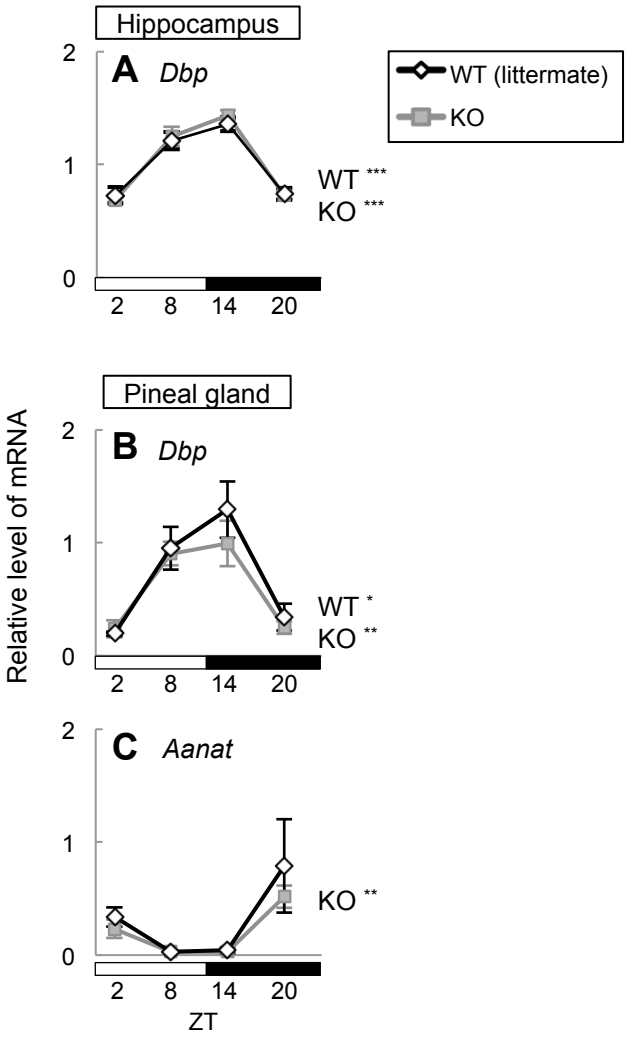

Figure 9 Expression profiles of mRNAs for clock related genes in the brain of *Cyp7b1* KO and the littermate WT mice

The oscillations of mRNA expression for clock related genes were investigated by RT-qPCR analysis of RNA samples prepared at four time points. (**A**) *Dbp* in the mouse hippocampus. WT***, KO***. (**B**) *Dbp* and (**C**) arylalkylamine *N*-acetyltransferase (*Aanat*) in the mouse pineal gland. *Dbp*; WT*, KO**. *Aanat*; KO**. Pineal glands of three mice were pooled at each sample. Data are normalized by mRNA levels of *Rps29*. Values are shown as the mean ± SEM (n = 3-4). * $P < 0.05$, ** $P < 0.01$, *** $P < 0.001$ by one-way ANOVA.

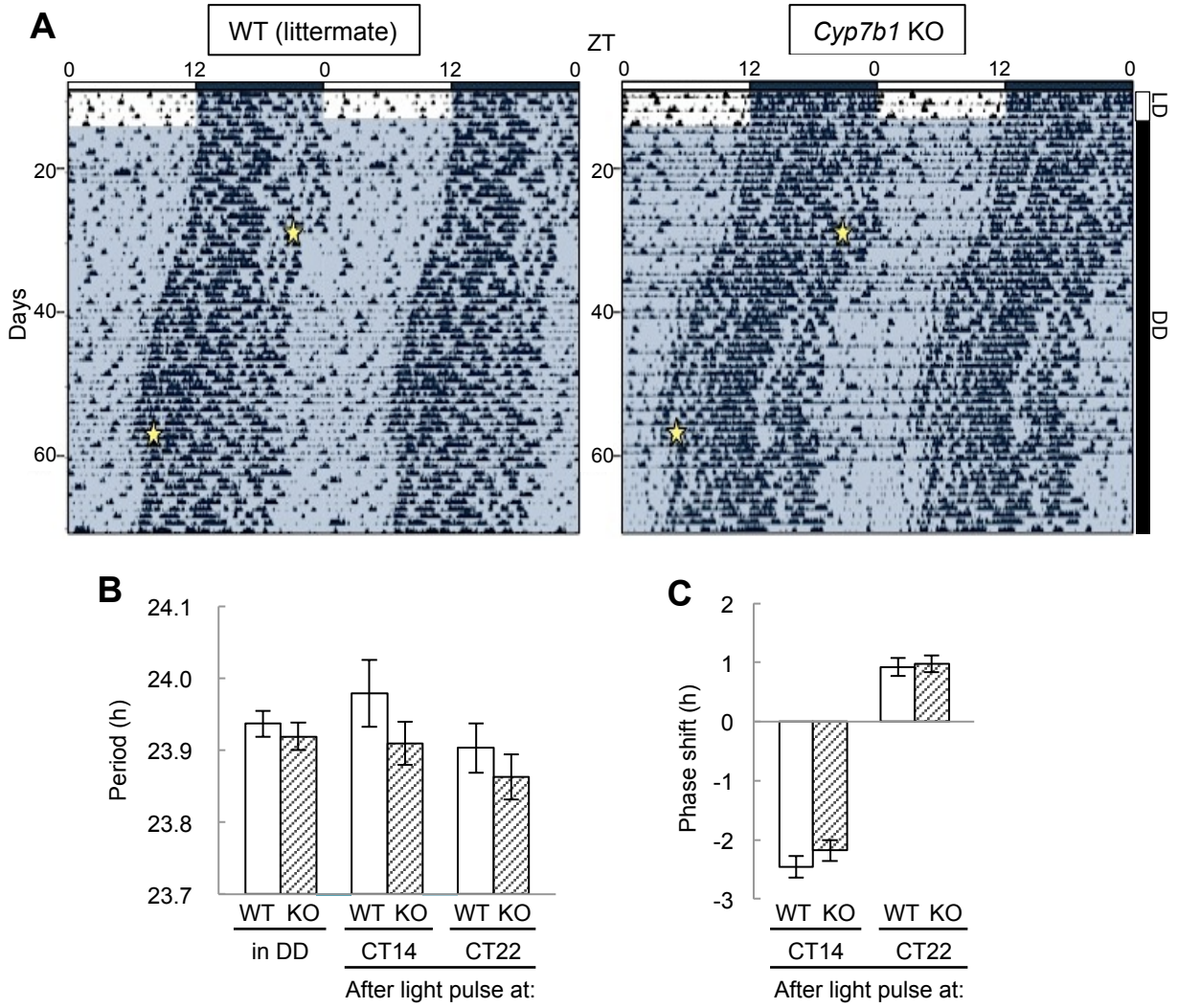

Figure 10 Locomotor activities and circadian periods of *Cyp7b1* KO mice and the littermate WT mice in constant darkness

Cyp7b1 KO and the littermate WT mice were entrained to 12 hr light/dark cycle (LD) and transferred to constant darkness (DD). Their free moving locomotor activities were monitored using infrared area sensors. (**A**) Representative locomotor activity records for *Cyp7b1* KO and the littermate WT mice in a double-plot format. Each onset in DD was defined as circadian time (CT) 12. Stars in actograms indicate the time points when a 30-min light pulse was given, at CT22 and CT14. (**B**) Circadian periods were calculated from actograms by extrapolation method before or after the light pulse. (**C**) Phase shifts in response to a 30-min light pulse. Phase of locomotor activity was delayed after the light pulse at CT14 (WT, -2.45 ± 0.19 h; KO, -2.18 ± 0.18 h) and advanced after the light pulse at CT22 (WT, 0.93 ± 0.15 h; KO, 0.98 ± 0.14 h). In B-C, values are calculated from the activities in 14 days for each mouse and shown as the mean ± SEM (WT, n = 15; KO, n = 14).

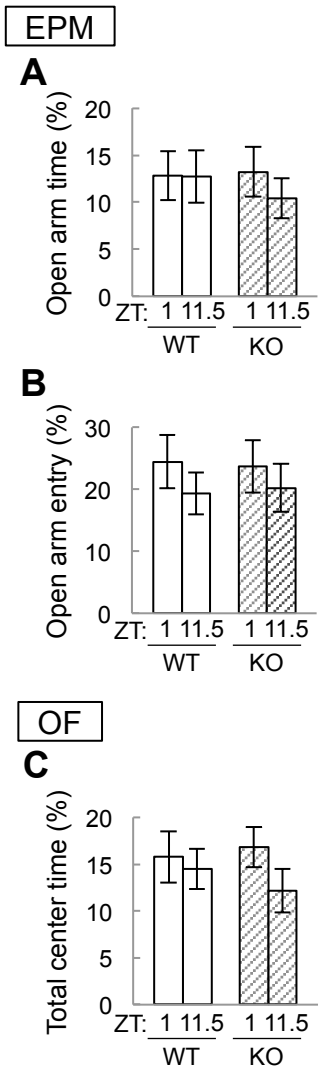

Figure 11 Diurnal expressions of emotional behaviors in *Cyp7b1* KO mice

Elevated plus maze (EPM) test and open field (OF) test were conducted at 2 time points, ZT1 or ZT11.5. Each mouse was subjected to all or part of these behavioral tests about emotion in the following order at least every second day. EPM test: (**A**) time ratio spent in open arms and (**B**) ratio of number of open arm entries (WT, *n*=16 for ZT1, *n*=16 for ZT11.5. KO, *n*=10 for ZT1, *n*=14 for ZT11.5.) OF test: (**C**) time ratio spent in center area (WT, *n*=12 for ZT1, *n*=17 for ZT11.5. KO, *n*=11 for ZT1, *n*=17 for ZT11.5.) Values are shown as the mean ± SEM.

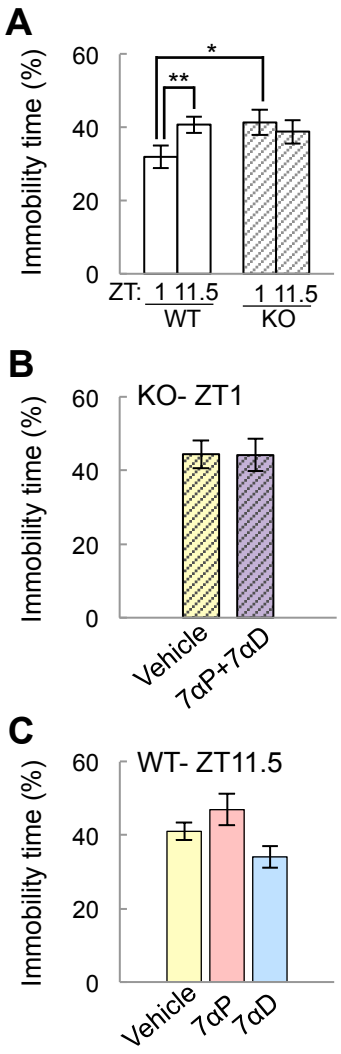

Figure 12 Forced swim tests in the dawn and the dusk in *Cyp7b1* KO mice

Immobility time in forced swim test. (**A**) Forced swim test was conducted at 2 time points, ZT1 or ZT11.5, and the immobility time in 5 min was expressed as percent ratio (WT at ZT1, n=24; WT at ZT11.5, n=30; KO at ZT1, n=20; KO at ZT11.5, n=22). * $P < 0.05$, ** $P < 0.01$ by Student's t test. A mixture of 7α-OH-Preg and/or 7α-OH-DHEA or 1% DMSO in aCSF (vehicle) was injected into the brain of mice transiently using syringe, and 10 min after the injection, the mice were subjected to the forced swim test. *Cyp7b1* KO mice at ZT1; (B) immobility time ratio in FS test. (n=12 for vehicle. n=12 for 7αP+7αD.) WT mice at ZT11.5; (C) immobility time ratio in FS test. (n=11 for vehicle, n=10 for 7αP, n=10 for 7αD.) Values are shown as the mean ± SEM.

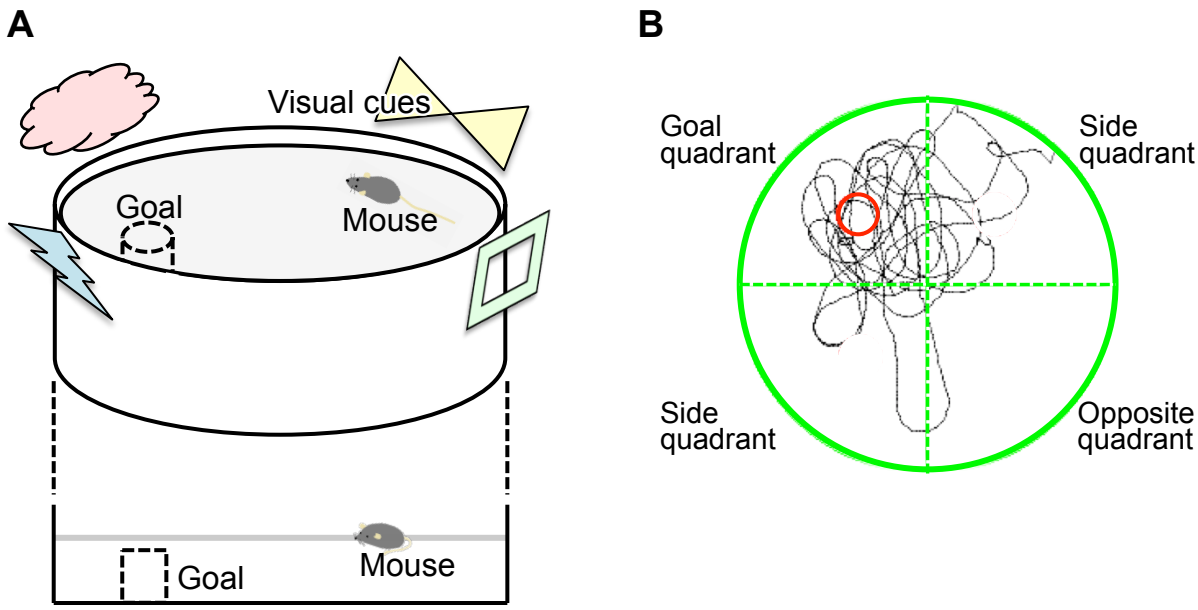

Figure 13 Image of the Morris water maze test

(**A**) The setting of the Morris water maze test. The Morris water maze test was performed in a circular pool filled with opaque water. A circular escape platform was placed below the water surface at a fixed position. In training trials, a mouse explored the hidden platform. After training trials, each animal was subjected to a probe test, in which the hidden platform was removed, and a time spent in exploring the platform (goal) quadrant, opposite quadrant, and side quadrants were measured for 1 min. (**B**) Representative trace of swimming in probe test. Small red circle; platform position, large green circle; pool.

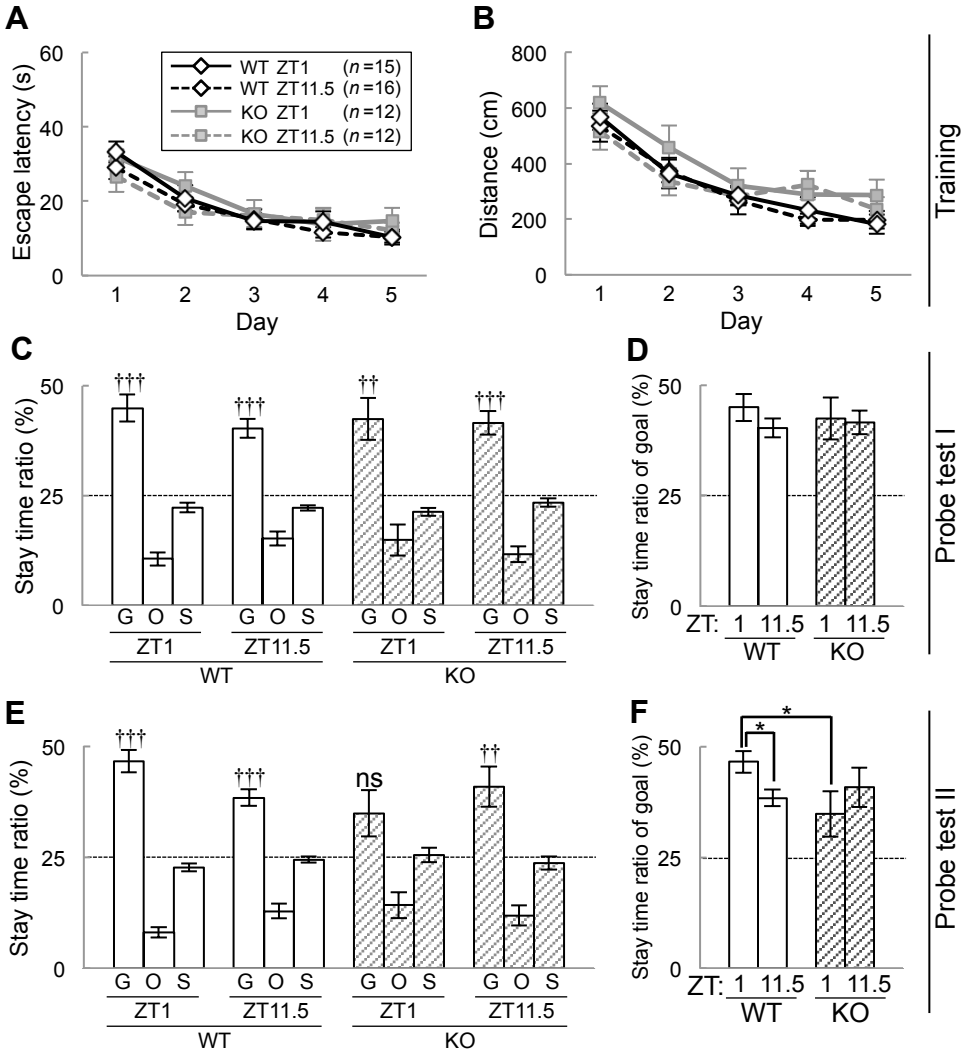

Figure 14 Spatial memory formation in Morris water maze test of *Cyp7b1* KO mice

Cyp7b1 KO and the littermate WT mice were subjected to the Morris water maze test at two time points, ZT1 or ZT11.5. The training trials (four trials/day) were performed for five consecutive days. (**A**) Average escape latency (sec) to reach the hidden platform and (**B**) average swimming distance (cm) in the training. Probe test I was performed on the next day of the last training (**C**, **D**). Probe test II was performed after two weeks from the probe test I (**E**, **F**). In these probe tests, the hidden platform was removed. (**C**, **E**) Stay time ratio (%) in total of 60 sec in G, goal quadrant, O, opposite quadrant, and S, side quadrants (stay times in the two S were averaged). Marks above the bars of G indicate *p*-values by Student's *t* test *versus* chance level (25%). † $P < 0.05$, †† $P < 0.01$, ††† $P < 0.001$, ns; not significant. (**D**, **F**) Stay time ratio (%) in G were compared among the four groups. * $P < 0.05$, ** $P < 0.01$ by Student's *t* test. Values are shown as the mean ± SEM (WT at ZT1, *n*=15; WT at ZT11.5, *n*=16; KO at ZT1, *n*=12; KO at ZT11.5, *n*=12).

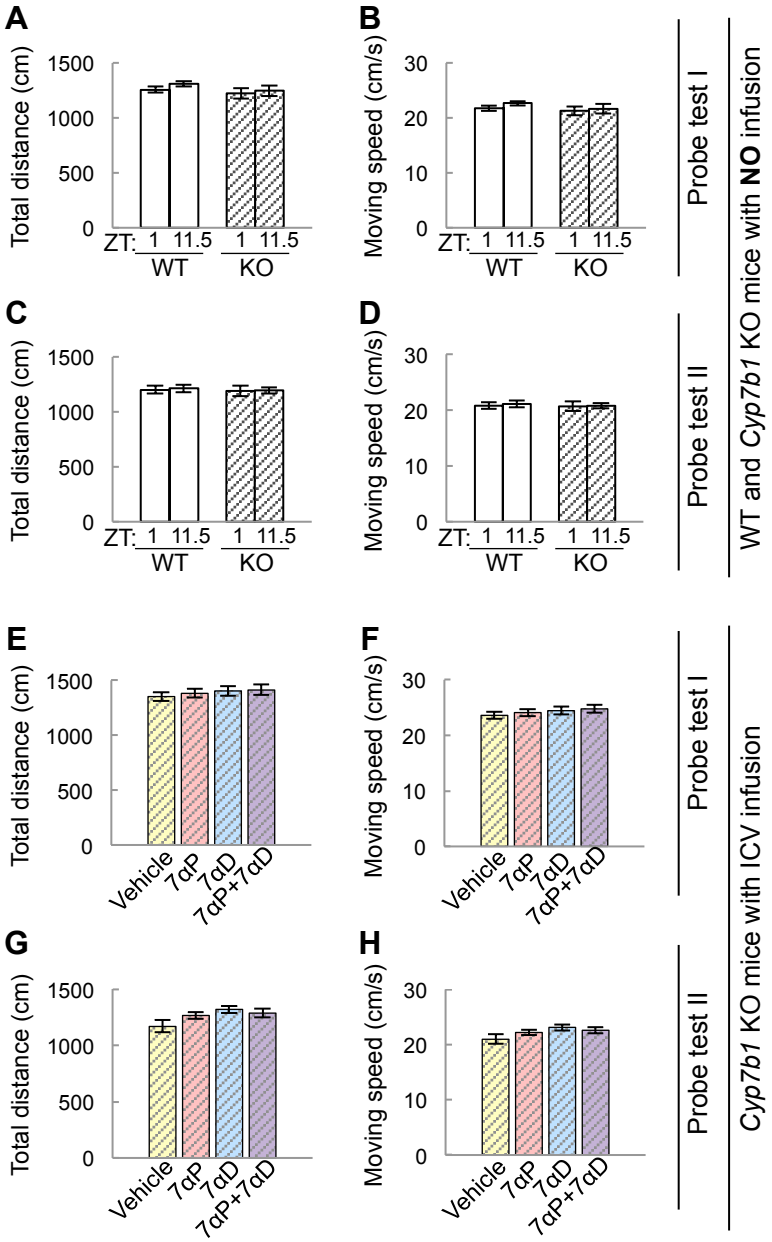

Figure 15 Activity parameters in probe tests of Morris water maze test

Total distance (**A**, **C**, **E**, **G**) and moving speed (**B**, **D**, **F**, **H**) of mice in probe tests of Morris water maze test (Figure 4, 5). Activities of (**A**, **B**) probe test I and (**C**, **D**) probe test II for *Cyp7b1* KO and the littermate WT mice in Figure 4. Not significant by Student's *t* test ($P>0.05$). Activities of (**E**, **F**) probe test I and (**G**, **H**) probe test II for *Cyp7b1* KO mice with ICV infusion of steroids in Figure 10. Not significant by Dunnett's test *versus* vehicle ($P>0.05$). Values are shown as the mean ± SEM.

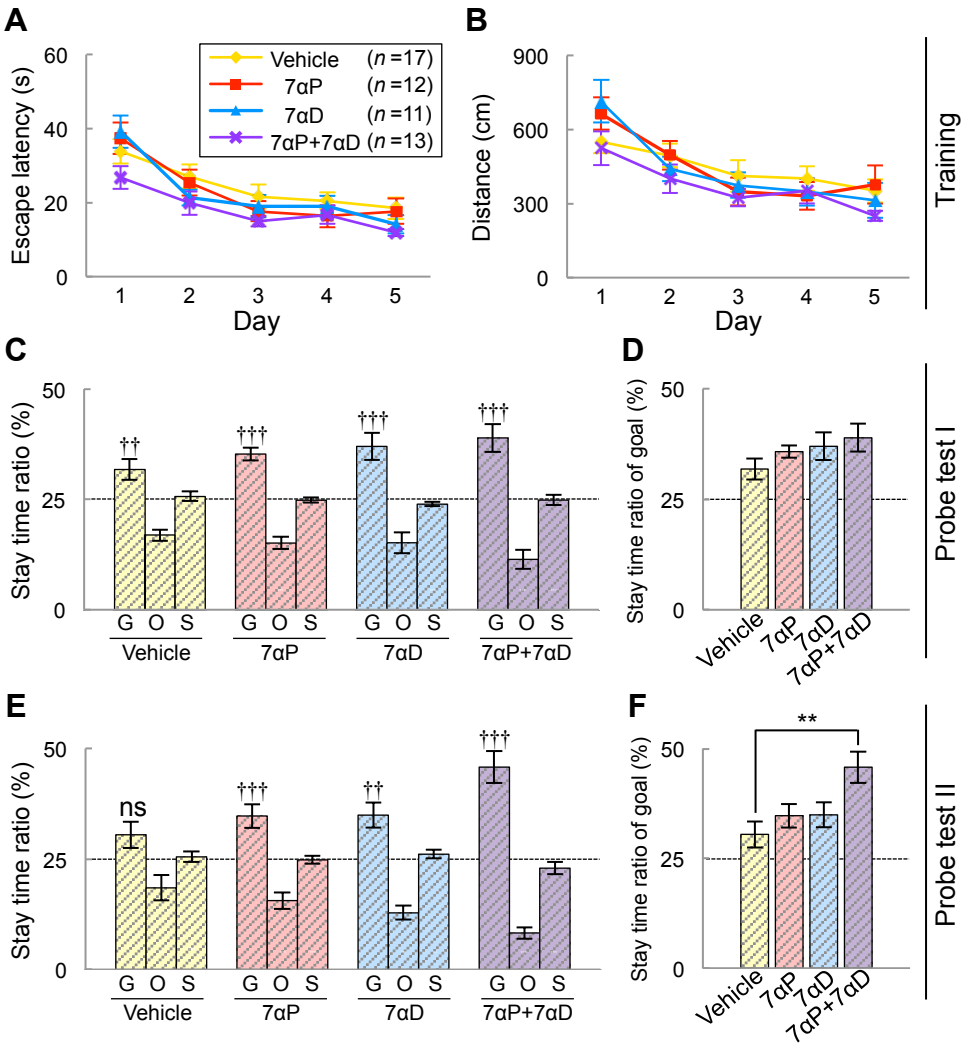

Figure 16 Effect of infusion of steroids on spatial memory formation in Morris water maze test of *Cyp7b1* KO mice

7α-OH-Preg and/or 7α-OH-DHEA were infused to *Cyp7b1* KO mice, and they were subjected to the Morris water maze test at ZT1. The training trials (four trials/day) were performed for five consecutive days. (**A**) Average escape latency (sec) to reach the hidden platform and (**B**) average swimming distance (cm) in the training. Probe test I was performed on the next day of the last training (**C**, **D**). Probe test II was performed after two weeks from the probe test I (**E**, **F**). In these probe tests, the hidden platform was removed. (**C**, **E**) Stay time ratio (%) in total of 60 sec in G, goal quadrant, O, opposite quadrant, and S, side quadrants (stay times in the two S were averaged). Marks above the bars of G indicate *p*-values by Student's *t* test *versus* chance level (25%). † $P < 0.05$, †† $P < 0.01$, ††† $P < 0.001$, ns; not significant. (**D**, **F**) Stay time ratio (%) in G were compared among the four groups. ** $P = 0.0020$ by Dunnett's test *versus* vehicle. Values are shown as the mean ± SEM (vehicle, n=17; 7αP, n=12; 7αD, n=11; 7αP+7αD, n=13).

8. Acknowledgements

I would like to show my greatest appreciation to my supervisor, Professor Yoshitaka Fukada, for his constructive and valuable discussion. I appreciate Dr. Kimiko Shimizu for her helpful comments and advice for experimental techniques. I am grateful to Dr. Tomoko Ikeno and Ms. Yoriko Mawatari for their help with behavioral experiments. I thank Dr. Daisuke Kojima, Dr. Hikari Yoshitane, and the other members of Fukada laboratory for their meaningful advice and pleasant days. This study was achieved by collaborations with Professor Toshifumi Takao and Ms. Qiuyi Wang for mass spectrometry. Finally, I would like to thank my family and friends for their warm encouragement.